Carbon Dioxide Enabled Methane Dehydroaromatization Reaction with High Stability

A Thesis

Presented in Partial Fulfillment of the Requirements for the

Degree of Master of Science

with a

Major in Chemical Engineering

In the

College of Graduate Studies

University of Idaho

by

Mark W. Hull

Approved by

Major Professor: Vivek Utgikar, Ph.D.

Committee Members: Eric Aston, Ph.D.; Hanping Ding, Ph.D.

Department Administrator: Dev Shrestha, Ph.D.

December 2021

Abstract

Benzene has been found to be used in over sixty percent of all industrially made chemicals. However, with a societal desire to be less dependent on fossil fuels, this unknowingly hurts benzene production. Although there are other alternatives to making benzene, methane dehydroaromatization proves to be the most efficient option. There have been many studies about MDA, however, few studies have been conducted to show that gas additions can improve the reaction. One study went over the effects of a carbon dioxide addition within the gas stream. The study showed that carbon dioxide is in competing nature with methane but stabilizes the reaction to a small degree. The work conducted in this report is to give a more detailed account of how carbon dioxide affects the MDA reaction. Carbon dioxide can increase the reaction's lifetime by over 700% (55-60 hours) but is most effective when its reaction time is held just above 20-25 hours (200% lifetime increase). With a carbon dioxide addition of 3 vol%, the reaction can keep a benzene selectivity of over 70% for its 25 hour lifetime. Of all the carbon dioxide values tested, 3 vol% addition provided the best results in terms of maintaining high conversion (~15%) and the highest selectivity (>70%). Carbon dioxide's role was theorized to help stabilize the reaction by transforming methane into a more reactive species: methanol. Using temperature programmed desorption, it was also theorized that propyne is the main reactant in forming benzene. Propyne polymerization is a well-known process, and it was theorized since propyne is the major product found on the catalyst's surface that propyne polymerization occurs to create mesitylene. Mesitylene is then hydrocracked to form methane and benzene. Further investigations revealed that carbon dioxide has the properties of arc quenching. This allows it to absorb free electrons without altering its physical chemistry. It was finally theorized that with a 3 vol% carbon dioxide addition, the optimal ratio of oxygen addition to electron removal of the reaction can be achieved.

ACKNOWLEDGEMENTS

I would first like to thank my major professor, Dr. Vivek with all the help he has provided with my thesis and my degree. He has been a tremendous resource and help in understanding how to write a well written thesis as well as helping guide me through the process of earning this degree. He's also been extremely helpful in explaining every pathway I could take to earn my degree. Without Dr. Vivek, earning my degree would have been much harder to accomplish.

I would also like to thank my lead researcher at Idaho National Laboratories, who also agreed to be on this committee, Dr. Hanping. Without his help and guidance, my research would have been a lot less focused and lacked the direction it needed from a more experience researcher. I'd also like to thank all his help with the writing of my thesis. He helped elevate my writing to a much higher standard. With his help, he not only let my research become much more focused, but also helped my writing to become much greater.

Finally, I would also like to thank Dr. Aston for his constant support throughout my degree. He has been crucial in helping me understand the program and how the system works at the University of Idaho. Without his constant effort and help from the very beginning, I would not be here today earning my master's degree.

DEDICATION

I would also like to thank my family for their help throughout the years of my education. I would especially like to thank my mom and dad Laura and Mahlon Hull for their constant help and support throughout my schooling. If it weren't for my mother, I don't think I would have been able to get through the tough times of school and have been able to achieve this goal. If it weren't for my father, I don't think I'd be able to do half the work that I am able to do right now. I would also like to thank my brother and sister: Mahlon Vaughn and Kathryn (Katie). If it weren't for my brother, it would have been much harder to see the smaller details that make things work. If it weren't for my sister constantly pushing me forward, I don't think I'd be able to have the drive to make it to the heights that I am able to achieve. I would also like to thank my grandparents: Darrel and Jan Gadbois as well as Dan and Eleanor Hull. Although grandpa Dan passed away many years ago, if it were not for all their love and care, it would not have been possible for me to finish any of my achievements that I have currently completed or will complete in the future.

TABLE OF CONTENTS

TABLE OF FIGURES

CHAPTER 1

Introduction to Methane Dehydroaromatization

1.1 Benzene: A Dwindling Resource

    Benzene is an important chemical in day to day life for most people. Benzene is primarily used in plastics, but it is also used in synthesizing medical drugs such as penicillin/ penicillin derivatives, the dyes that impart color to our clothes, and industrial lubrication.[1] Without benzene, most major industries would no longer be able to function. Benzene is a special hydrocarbon as it consists of three alkene bonds within a 6-carbon ring, forming the basic structural unit of an aromatic compound. This structure imparts it stability while also providing many pathways for reactions. However, benzene is becoming a more scarce resource every day. Benzene is the main byproduct from fossil fuel refinement.[2] When refining crude oil, the long polymer chains that form the oil must be broken down into a usable form. This can be done at high temperatures above $300\ °C$ ($572\ °F$) and with a silver
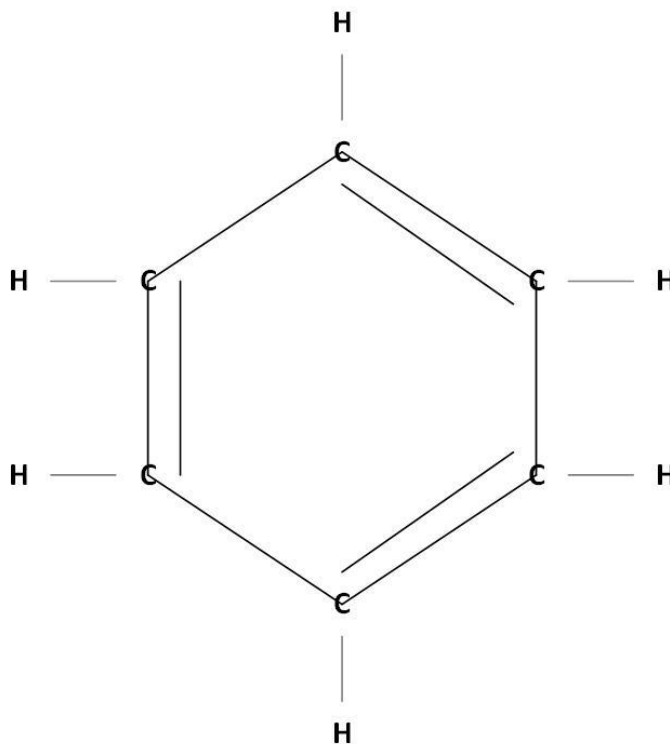
Figure 1: Model of Benzene Molecule

catalyst and a zeolite support structure. Although benzene is the main aromatic component in oil, it can also be formed from other secondary byproducts. These byproducts are light alkanes that are also created when breaking down the same crude oil. These light alkanes have limited use and must be transformed into a usable product. Therefore, most light alkanes formed by this process are turned into benzene. However, with the recent changes in society mentality, people have decided to become more green with their habits. This has included replanting forests, driving hybrid/electric cars, and transitioning away from fossil fuels. Because of this, benzene production, along with gasoline production, will decrease causing benzene products to become more expensive over time. Although there are more natural ways of acquiring benzene, the uses for it are so vast that it could not keep up with demand. An alternative must be found.

1.2 Methane: A Wasted Resource

Methane poses a large problem for not only benzene, but for the planet as well. Although the Earth is very abundant with methane, as shown by a US government report tracking the gaseous atmospheric concentration of methane, most methane that is bought and

Figure 2: Active Lights at Night in the United States Krulwich, Robert. "A Mysterious Patch of Light Shows up in the North Dakota Dark." National Public Radio, https://www.npr.org/sections/krulwich/2013/01/16/169511949/a-mysterious-patch-of-light-shows-up-in-the-north-dakota-dark

sold is found in the farming and petroleum industry.[3,4] Methane is the main byproduct from living animals such as cows and pigs. These animals emit methane gas where it can be harvested and sold. However, with a large population and the amount of pork and beef consumed every year increases, the amount of methane produced is increasing exponentially. However, both industries cannot simply capture and sell all the methane being produced. It would not only render methane worthless, but it would also destroy many industries that depend on methane. One of these industries is hydrogen production. Therefore, methane must be reduced to stabilize its price within the market. This leads to a 2013 article by the National Public Radio.[5] In 2013, the NPR presented a photograph of the United States at night. This photograph showed the light generation differences between the east and west coast of the United States. However, in North Dakota, they discovered that so much methane is being produced that the only way to reduce it is to burn it. This burning of methane produces tons of carbon dioxide every year. As stated earlier, when crude oil is refined, light alkanes are created, namely, methane, ethane, and propane. Although methane can be transformed into benzene through a process called indirect methane conversion, it is far easier for ethane and propane to be transformed into various aromatics such as benzene. It is much harder for methane to transform into benzene because of its simplistic nature. Because methane is a singular carbon bonded to four hydrogens, it is very unstable when trying to react and form into longer hydrocarbon chains. Therefore, it is necessary to change methane into a more reactive species. This is usually in the form of methanol (methane with an alcohol group). However, this is difficult to achieve as the process, called steam reforming, wants to produce carbon monoxide rather than methanol. However, partial oxidation of
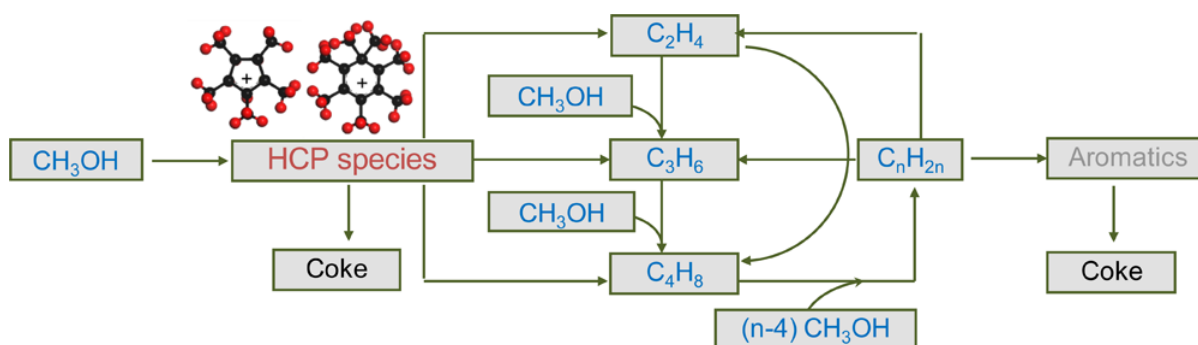
Figure 3: Methanol to Aromatic Process *"Methanol to Olefins (MTO): From Fundamentals to Commercialization." ACS Catalysis, vol. 5, no. 3, Mar. 2015, pp. 1922–38. DOI.org (Crossref), https://doi.org/10.1021/acscatal.5b00007*

methane can transform methane to methanol, but it requires more steps to complete. Namely it requires a zeolite supporting structure with a catalyst that can perform the reaction, such as SSZ-13 and a copper catalyst. *Figure 3* depicts a typical process of creating benzene with methanol and other light alkanes. Although this may seem like a promising way to produce benzene, since methane production is very heavily created in the petroleum industry, it would not serve as a long term solution. This is due to benzene being a secondary product to the gasoline that is created. Therefore, creating benzene using methane that is cheaper and more effective is needed. Then in 1993 a researching group led by Linsheng Wang found a more direct way. Instead of reforming light alkanes into benzene in less than ideal conditions, they can be directly converted under appropriate catalyst action directly into benzene.[6] This process is called methane dehydroaromatization (MDA), discussed in more detail below.

1.3 Methane Dehydroaromatization: The Critical Reaction

MDA was first discovered in 1993 by Wang and his coworkers.[6] The goal of their study was to find a way of converting methane directly into benzene. This was done with multiple catalysts, but the most prominent was molybdenum. The reaction can be found by looking at *Equation 1*:

$$6CH_4 \rightarrow C_6H_6 + 9H_2 \hspace{3cm} \textit{Equation 1}$$

This process provides a much needed service for not only the benzene industry, but for greener initiatives as well. This process increases the value of methane by reacting it into a more valuable chemical. As of right now, methane's primary use is to turn into hydrogen gas. However, the amount of methane generated exceeds the amount of hydrogen needed. Therefore, methane is burned to help stabilize its price within the market. With this reaction, methane will become a more desirable product as it can directly convert into aromatics with high value. This process also decreases the value of benzene and other aromatics. Benzene will no longer be as hard to make and become more abundant within the industry. This will cause the value of more complex chemicals to become cheaper and make the processes to make them simpler, which will inherently make them not only safer but more economic as well. Although commercialization is the intended goal, there are many problems associated with this reaction. This reaction has a lifetime of only seven hours on average. This is a very

short lifetime in comparison to other processes. For example, a catalytic converter in vehicles has a lifetime of approximately 10 years. Imagine if a catalytic converter would need to be replaced every 1000 miles. This would be very inconvenient as well as expensive. The same can be said for the catalyst used in MDA. Therefore, the lifespan of the catalyst must be increased before it could be used industrially. Another problem for this reaction is the temperature and coking of the catalyst. This process is an endothermic process and requires temperatures of up to $700\ ^{\circ}C$ for the reaction to take place. This high temperature is due to the unstable nature of methane. For methane to transform into larger hydrocarbons, the molecule must lose a hydrogen and react via carbocation, a positively charged carbon reaction. This causes instability to the molecule as hydrogen cannot donate nor shift its electrical charge to help balance the positively charged carbon. Therefore, the reaction becomes spontaneous. This also leads to the coking problem. Reactions that require carbon rearrangement and or carbon-carbon interactions, have the possibility of turning into coke. Coke is a large carbon structure that has high stability and low value. Coke can come in two different forms depending on the temperature. At temperatures below $300\ ^{\circ}C$, coke primarily consists of a non-aromatic form usually as graphene. At temperatures above $400\ ^{\circ}C$, coke primarily consists of a multiple benzene rings bonded together called polyaromatic hydrocarbon (PAHs). Although both forms of coke are problematic for their respective temperatures, graphene does have some practical application such as a printer powder. However, PAHs do not have any practical application. This is because of not only its properties, but also because of its highly stable nature. This stable nature is because of its ability to delocalize its electrons to other aromatic rings within its compound. This causes the coke to become non-reactionary in most conditions. However, it is possible to break apart the bonds and reduce the structure back to benzene. However, the cost to turn it back into benzene is far greater than the price of benzene. Therefore, it is more economical to dispose of it. Because of these problems, MDA has been continuously researched for over 25 years to determine the best conditions for the reaction to take place. Most research can be classified into three major groups: the catalyst, the zeolite, and the gas stream.

Most catalyst research for MDA is primarily focused on changing the primary catalyst, rather than the environment that the catalyst is found in. However, some studies

have been focusing on altering the dispersion of the catalyst on the zeolite, altering the pH of the catalyst, or other such effects. Most catalyst research has gone into developing one of two major portions of the catalyst: the primary catalyst and or the promoter (secondary) catalyst. The molybdenum catalyst was the initial finding of Wang et al. in 1993.[6] However, since the initial findings, there have been few other catalysts that have performed as well as the molybdenum catalyst. One catalyst that showed some promise was an iron catalyst. Because of iron's low value, it is an easily replaceable catalyst, and it does not matter (as much) if the catalyst deactivates via coke buildup. However, there have been many studies on iron catalysts that have shown that it does not perform well in this reaction. One such study was conducted by Denardin & Perez-Lopez.[7] The research looked at various iron catalysts with different promoters. Some of these promoters were molybdenum, niobium, and zirconium. The best performing catalyst was a basic iron catalyst that achieved 3.3% methane conversion after 360 minutes. The selectivity to benzene was only 45% and the selectivity to coke was 43%. In comparison to an average molybdenum catalyst, methane conversion is within 15-18% and the benzene selectivity is approximately 85%. Although the paper determined some differing effects with zirconium and niobium within the MDA reaction, the iron catalyst underperformed in every category. Therefore, it was assumed that an iron catalyst could not perform in this reaction. However, in a 2021 study, it was shown that an iron catalyst can perform in the MDA reaction. According to Gu et al., an iron catalyst can perform, but only under specific conditions.[8] It is well known that metals can have two electronic states, and iron is one of them. The research determined that while the reaction was converting methane into benzene, the iron catalyst would not shift back to its original electronic state of 3+ but would instead degrade to 2+. This causes iron to have a lower methane conversion and benzene selectivity. Promoter catalyst research is far simpler as it only requires a well-researched catalyst, such as molybdenum, and a metal that could also be used within the reaction. This is usually reserved for more expensive catalysts such as gold and platinum. Therefore, most research was catered towards the precious metals, but there are some studies that focus on other promoters such as copper and calcium. One such study was done by Denardin and Perez-Lopez.[9] Some of the promoters used were magnesium, calcium, zinc, copper, nickel, cobalt, and lanthanum. Most of these promoters

did not perform well, however, both calcium and copper decreased the amount of coke produced on the catalyst.

There has been very limited zeolite research because of the nature of Zeolite Socony Mobil-5 (ZSM-5). ZSM-5 is ideal for this type of reaction as it has a dual pore size of 5.5 Å/5.6 Å. This is the ideal size of the benzene molecule, and thus it limits the size of any aromatic to be benzene or a small derivative of benzene. It is also ideal as it is inexpensive to make. However, there is a similar zeolite called Mobil Composition of Matter No. 22 (MCM-22) that can also perform well within the reaction. Therefore, most zeolite research is catered to making the current zeolites better by reorienting them or to create a new zeolite. Although it seems promising to use a new zeolite, they usually underperform and are far more expensive. This can be seen in Wang et al.'s paper about using a grass ball catalyst with a ZSM-5 zeolite.[10] The research concluded that limiting the transfer mechanics (i.e., diffusion) allowed more molybdenum to become activated, but did not change the fundamental problems of the reaction (i.e., coking).

The final area of research is the gas stream. This is the least popular option as changing the gas stream does not change the physical properties of the catalyst nor the zeolite. Therefore, research is very limited. There has been some research, by a few groups, but one group is the most referenced. Ohnishi et al., is the main referenced group as their research showed how an addition of carbon monoxide & carbon dioxide can alter the reaction towards benzene.[11] The research took place at Hokkaido University and the major findings are discussed below.

1.4 Previous Work Findings of Carbon Dioxide

As previously discussed, methane transforming into aromatics can take place in many ways. MDA is one of the only methods that is performed under non-oxidative conditions. This was revolutionary as up until that point, methane could only turn into aromatics through indirect methods. However, MDA allowed this process to happen directly without the use of oxygen. Ohnishi et al., were one of the first researchers to add oxygen into the reaction to discover how it worked within MDA. This was accomplished by adding in a set amount of carbon monoxide or carbon dioxide. The purpose of this research was to discover how

adding in both carbon and oxygen affected MDA and the resulting products. The research concluded that both carbon monoxide and carbon dioxide are both used within the reaction and produce more aromatics. However, carbon dioxide has a secondary competitive reaction. This reaction produces carbon monoxide that can also be used within the MDA reaction. Their work can be seen in Appendix A, *Figure A 58 & Figure A 59* for their baseline molybdenum conversion and their carbon dioxide research. To help determine what was found on the catalyst, the research employed temperature programed oxidation (TPO) to determine the types of organics that are found. TPO is a process in which a spent catalyst is heated up with oxygen. The purpose of TPO is to determine the number of organics found on a catalysts surface by oxidation. Ohnishi et al. used TPO to measure the amount of coke left on the catalysts surface. Their results concluded that they would achieve ~10% methane conversion initially and the conversion would deteriorate over time. They also found that although benzene was the most abundant chemical created, they also had some amount of naphthalene, anthracene, and phenanthrene before it would transform into PAHs. Although benzene is the main product desired, naphthalene, anthracene, and phenanthrene are also acceptable byproducts. The research tested various volume percentages of both carbon dioxide and carbon monoxide (namely 1.4%, 4%, and 12.1%). As the volume percentage of carbon monoxide increased, a positive trend towards both benzene selectivity and methane conversion was shown. However, carbon dioxide showed the opposite effect. As the volume percentage of carbon dioxide increased, a negative trend towards both benzene selectivity and methane conversion was shown. However, this seems antithetical to logic. Therefore, a deeper dive into carbon dioxide and its effects on the reaction need to be studied as it can help further the understanding as to how MDA reacts with both methane and carbon dioxide.

1.5 Goals and Outcomes

The main goals of this study are to conduct a systematic study of the effect of carbon dioxide on MDA and expand upon the previous work. Carbon dioxide was chosen as it would help reduce the greenhouse gases, as well as show a potential localized maximum that optimizes methane conversion and benzene selectivity. The objectives for this work were to determine the effect that carbon dioxide has on the MDA reaction. This is done by

comparing the results with no carbon dioxide addition, baseline result, with results with carbon dioxide. The amount of carbon dioxide being tested would start at 1% addition by volume and increases by 1% for every new trial. This would continue until the outlet stream does not show any benzene selectivity or the catalyst was completely suppressed (whichever comes first). The selectivity to benzene, alkenes, and higher weight aromatics would also be determined. The next objective was to determine the most optimal carbon dioxide ratio. This was done by comparing the initial baseline conversion and selectivity to the carbon dioxide addition results. If the methane conversion or benzene selectivity was less than the methane conversion or benzene selectivity with carbon dioxide added into the stream, then that concentration would be optimal. The final objective was to explore the mechanisms found within the reaction and to theorize a reactionary pathway. This was achieved with temperature programmed desorption (TPD). TPD can be used to determine the chemicals on the catalyst's surface and show potential reactionary pathways to benzene.

CHAPTER 2

Experimental Work

2.1 MDA Testing

2.1.1 Data Acquisition

Use *Schematic 1* as a visual representation of the system. A gas chromatograph with an attached mass spectrometer, Shimadzu Nexis GC-2030 & GCMS-QP2020 NX , was implemented to determine the methane conversion and various selectivities of the catalyst. The system was calibrated to find ethane/ethene, benzene, and C_7+ hydrocarbons. The gas chromatograph was connected to a GSL-1100X standup furnace. A ~0.1 mm inside diameter glass tube reactor was inserted into the furnace to carry out the reaction. The gas would pass through the top of the furnace and onto a fixed bed reactor. This stream was then fed to the gas chromatograph. The exit stream was kept at a constant 130 $°C$ to ensure that the benzene would not condense on the side of the tubing.   The furnace was held between 700-730$°C$ to replicate the original experiment by Ohnishi et al. ALICAT and Parker flow meters were used to ensure that the flow rates of methane and argon could be controlled. The temperature was recorded and controlled by an OMEGA Thermocouple Probe (KMQSS-062U-24) using the NI Temperature Logger. An OmniStar ThermoStar (GSD320 Gas Analysis System) was used to determine the adsorbed molecules still on the catalyst's surface (TPD). An Agilent Technologies 7890A gas chromatograph with an attached Agilent Technologies 5975C inert XL MSD mass spectrometer was also used to measure activity of CO_2 within the reaction.
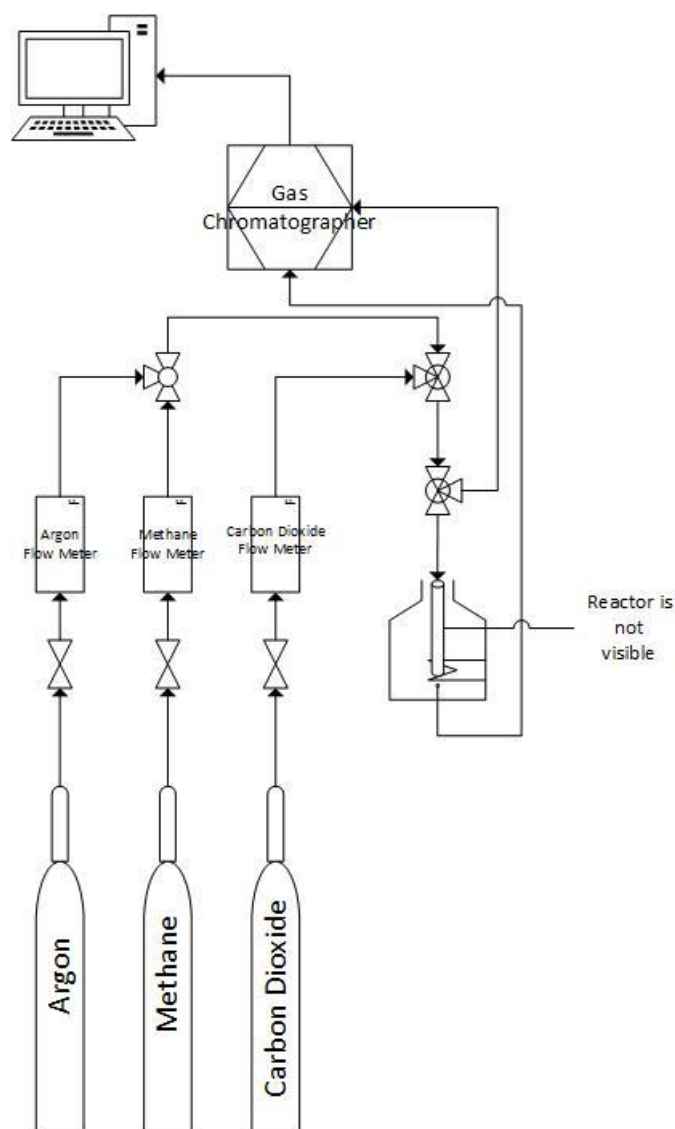
Schematic 1: Carbon Dioxide Testing Setup

2.1.2 Catalyst preparation

Molybdenum catalysts for each run was prepared by incipient wetness impregnation (IWI).[7,12–18] The zeolite used was HZSM-5 (Si/Al = 25, Zeolyst international, surface area 425 $\frac{m^2}{g}$). The molybdenum catalyst used was ammonium heptamolybdate tetrahydrate (AMT 99.3% purity). To create the catalyst, about 0.185 grams of AMT was dissolved in 3000 μL of deionized water. This solution was then put into an ultrasonic cleaner bath to break up the larger AMT particles, by suspension, to evenly disperse it. Five grams of HZSM-5 was

weighed and placed into a beaker. To ensure a solid impregnation not all 3000 μL were added in at once. To start, 200 μL of the solution was added into the zeolite using a micro pipette for the first 600 μL. For the rest of the solution, only 100 μL were added in per addition until all 3000 μL were put onto the zeolite bed. Any clumps within the zeolite bed were broken apart using a glass rod to ensure consistency within the dispersion after each addition. After impregnating, the catalyst was calcined at $120°C$ for 24 hours within an oven. The next day, it would then be placed within a furnace and would be heated to $700°C$ for 2 more hours with a constant air stream at 100 mL/min. This resulted in a 2% Mo/HZSM-5 catalyst which was the basis for the experiments.

2.1.3 Procedure

The procedure started by taking 0.5 grams of the molybdenum catalyst and placing it within the glass tube reactor. The glass tube reactor would then be placed in the furnace where 20 mL/min of argon would flow into the top of the furnace/reactor and flow down towards the gas chromatograph. As the argon is flowing, the furnace would be heated up to $700 - 715 °C$ using the thermocouple. This was to ensure that the catalyst was dried sufficiently, and surface chemicals were removed. Once the furnace had reached the operating temperature of $700 - 715 °C$, the argon flow was stopped and was replaced with a methane and nitrogen flow (95%/5% respectively) for the reaction. The flow rate of this stream was $10.64 \frac{mL}{min}$. The furnace was put into a bypass mode so that the gas chromatograph could measure the amount of methane within the stream. This was achieved by using a t-valve that would allow methane to "bypass" the glass reactor/furnace, so that only the non-reacted methane was fed into the chromatograph. This would be used to determine the amount of methane that reacted by first evaluating how much methane was being fed to the gas chromatograph. This bypass mode was done for ~75 minutes to ensure that the flow to the gas chromatograph was at steady state and that the gas chromatograph had an accurate reading. Once this was completed, the t-valve was put into its secondary position dubbed "reaction mode". In reaction mode, the methane feed was fed over the catalyst bed, so that it could react. This stream would then be sent to the gas chromatograph. There were three types of tests that were conducted over the course of the experiment: short,

medium, and long term trials. In short term trials, the methane stream was fed over the catalyst for approximately 1 hour. This was used to determine initial selectivities and conversions of the catalyst. In medium term trials, the methane stream was fed over the catalyst for approximately 7 hours. This was used to determine how quickly the catalyst was degrading in an average molybdenum lifetime. In long term trials, the methane stream was fed over the catalyst for approximately 12-15 hours, except in 1 vol% carbon dioxide addition where it was fed for over 60 hours. This was used to determine the long term methane conversion, selectivities, and stability of carbon dioxide over the molybdenum catalyst. The short term and medium term graphs can be found in Appendix B. Once the reactor was finished with the experiments, the reactor would be turned off and the sample stored in a quartz vial for long term storage after it was cooled.
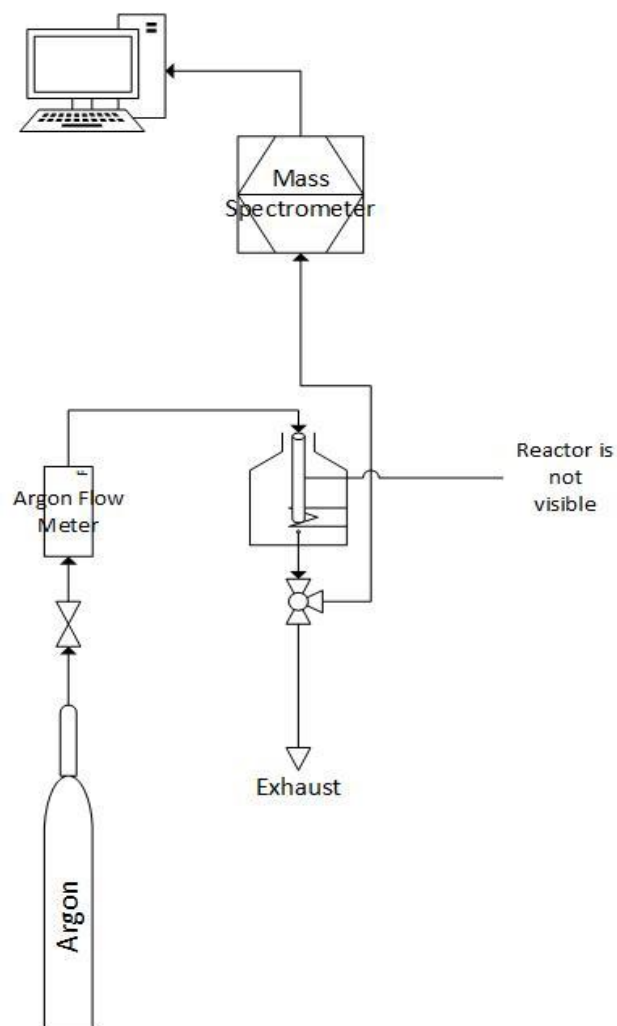
Schematic 2: TPD Testing Setup

2.2 Temperature Programmed Desorption Procedure

Use *Schematic 2* as a visual representation of the system. The pre or post reaction sample would be used for TPD. This was to study the characterization of the catalyst, as well as the mechanics of the reaction. The OmniStar ThermoStar (GSD320 Gas Analysis System) mass spectrometer was used for this process. When testing TPD, 0.1 grams of the fresh or spent catalyst is placed in a short glass tube reactor. The mass spectrometer must be turned on by first heating up the machine, then opening the inlet valve, then finally turning on the filament. Turning it off it must be done in the reverse order. This was to ensure that the filament within the mass spectrometer was not damaged during operation. The data acquisition starts by first opening the inlet value of the Argon gas allowing it to flow across the sample and into the mass spectrometer. A baseline acquisition needs to be taken to ensure that the mass spectrometer is working properly. This is done by turning on the mass spectrometer and making sure that the argon flow stream is at a steady ionic current. Once this baseline has been taken, the furnace can then be programmed to the desired final temperature and the time it takes to get to the final temperature. For the TPD experiments, the furnace was always set to its maximum allowable highest temperature, which was $860\ °C$. This would ensure that anything that could desorb on the catalyst would desorb. Next, the amount of time it takes to reach the final temperature is programmed. Generally, the slower the temperature rise, the more accurate the mass spectrometer will be. Based on other reports and coworkers, a $4-5\ °C$ per minute increase would be sufficient. Therefore, the total run time of the experiment would be 3.5 hours. During this time, both the ionic strength and temperature of the mass spectrometer were recorded for future use. After the allotted time and the final temperature has been achieved, the final temperature and ionic strength can be plotted against one another to create the TPD graphs found in Appendix A. This can be done using a Microsoft Excel program.

CHAPTER 3

Experimental Results & Conclusions

3.1 Carbon Dioxide Test Results

3.1.1 Baseline Conversion

In the MDA reaction, molybdenum catalysts with a HZSM-5 zeolite support structure are the most studied catalysts. The molybdenum catalyst that uses a HZSM-5 zeolite has an approximate 6-7 hour lifetime before complete deactivation. The conversion of this catalyst is dependent on a few factors, but if the weight percentage of molybdenum does not exceed 6%, the conversion will lie between 10% to 19%. Through many testings, 19% is the upper limit to this reaction. *Figure 4* shows the results of the baseline methane conversion tests with the catalyst outlined in Chapter 2. Although the conversion is on the high side, it is within the acceptable range for this type of catalyst. Poor dispersion of molybdenum metal can cause the catalyst to clump together within the zeolite. When this occurs, this can cause the conversion to be slightly higher than average, but also causes quicker deactivation. This can either cause one of two outcomes. Either the zeolite pathways become entirely blocked and the catalyst is deactivated, or most of the catalyst becomes deactivated, but some
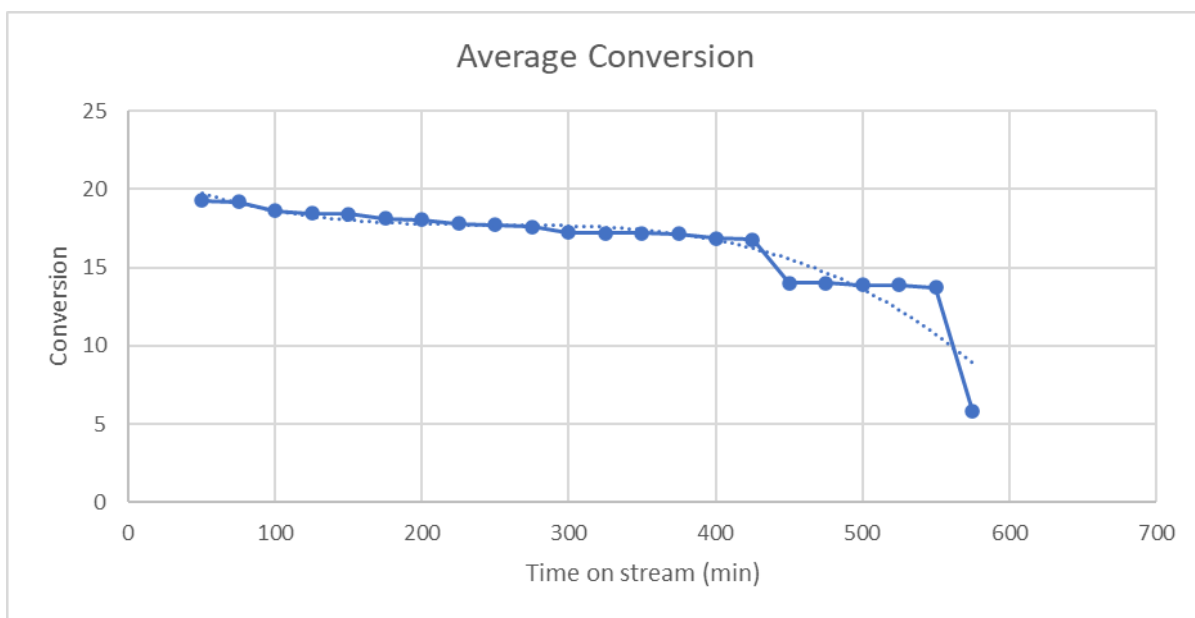

Figure 4: Average Baseline Conversion of Methane

pathways exist for the reaction to continue.[19] At the 450 minute mark there is a noticeable drop in conversion before complete deactivation. This is due to partial blocking of the zeolite pathway due to the catalyst clumping together. However, *Figure 4* is in line with other researchers.

3.1.2 Carbon Dioxide Addition Methane Conversion Results

With the baseline conversion completed, the effects of carbon dioxide can be quantitatively analyzed. The first step was to determine the "catalyst death" as it would limit how much carbon dioxide would need to be added within the gas stream. Looking at *Figure 5*, it was determined that a 5 vol% addition of carbon dioxide would be an appropriate stopping point. The two main factors for determining catalyst death are methane conversion & benzene selectivity. A low methane conversion doesn't necessarily mean catalyst death and neither does a low benzene selectivity. However, as seen in *Figure 6*, a 5 vol% addition leads to no benzene creation. Using both *Figure 5 & 6*, it can clearly be seen that a 5 vol% carbon dioxide addition does not produce adequate results. The average methane conversion for this gas addition is ~7%. Using the baseline conversion as the maximum (19%), this is a 60% efficiency loss. That is too high of a methane conversion loss to justify using anymore carbon dioxide. This is the point in which the catalyst is suppressed completely by carbon
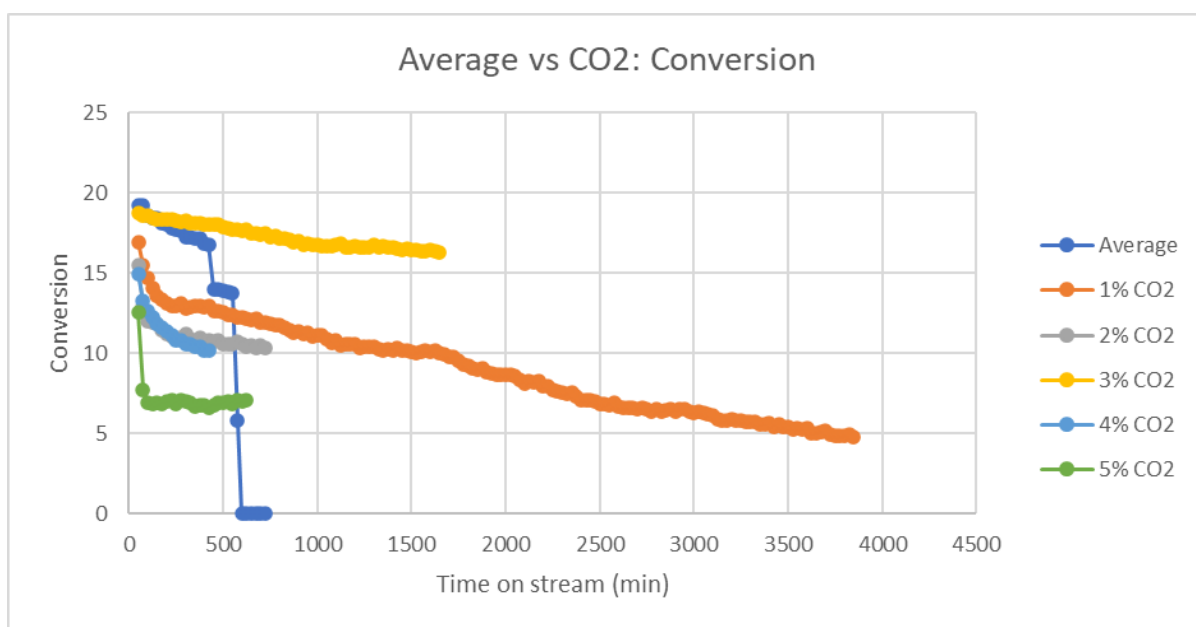

Figure 5: Average Baseline Conversion vs Conversion of Methane with CO_2

dioxide as shown by other reports.[11,20] This heavily limits our testing range and allows for a more comprehensive search for a potential methane conversion maximum or catalyst lifespan maximum. The first major testing point can be found in the 1 vol% carbon dioxide addition. This carbon dioxide addition was tested for over 60 hours. This was done to find the maximum lifetime of the catalyst. This resulted in a 750% increase to the catalyst lifespan compared to the average. However, as stated with a 5 vol% addition, a conversion that has over 60% efficiency loss is too much for this reaction. Therefore, an effective catalyst lifetime should be determined. Although it can be arbitrarily determined, a methane conversion of 10% is usually the stopping points of most researchers.[13,16,18,19] Using the same metric, it can be seen that the catalyst reaches 10% conversion roughly at 1500 to 1600 minutes. It can be proven that the effective catalyst lifespan is increased by 250% when using 1500 minutes (25 hours) as the new stopping point. Either case shows that some addition of carbon dioxide increases the catalyst's lifetime. This in turn increases the amount of methane reacting and benzene created. The second major testing point can be found in the 3 vol% carbon dioxide addition. The conversion with a 3 vol% addition exceeds the baseline conversion after 250 minutes of reacting. In every experiment, except for 4 vol% carbon dioxide addition, the catalyst has a longer reacting time than the baseline catalyst. However, in each carbon dioxide trial, the conversion is always lower than the baseline conversion, except in a 3 vol% addition. Although the conversion is initially less than the baseline conversion, a 3 vol% addition allows methane to continue reacting at a high conversion than any other trial. For methane conversion, a 3 vol% addition is the local maximum.

3.1.3 Benzene Selectivity

As stated in the previous section, the methane conversion and benzene selectivity are critical in determining the effectiveness of carbon dioxide addition. *Figure 6* shows the results of the carbon dioxide additions. As mentioned before, a 5 vol% addition shows why it was the "catalyst death". The benzene selectivity of the addition never reaches above 10%, which is extremely poor for this reaction. The goal of MDA is to turn methane into more valuable products. Although this does not necessarily mean benzene, more information on
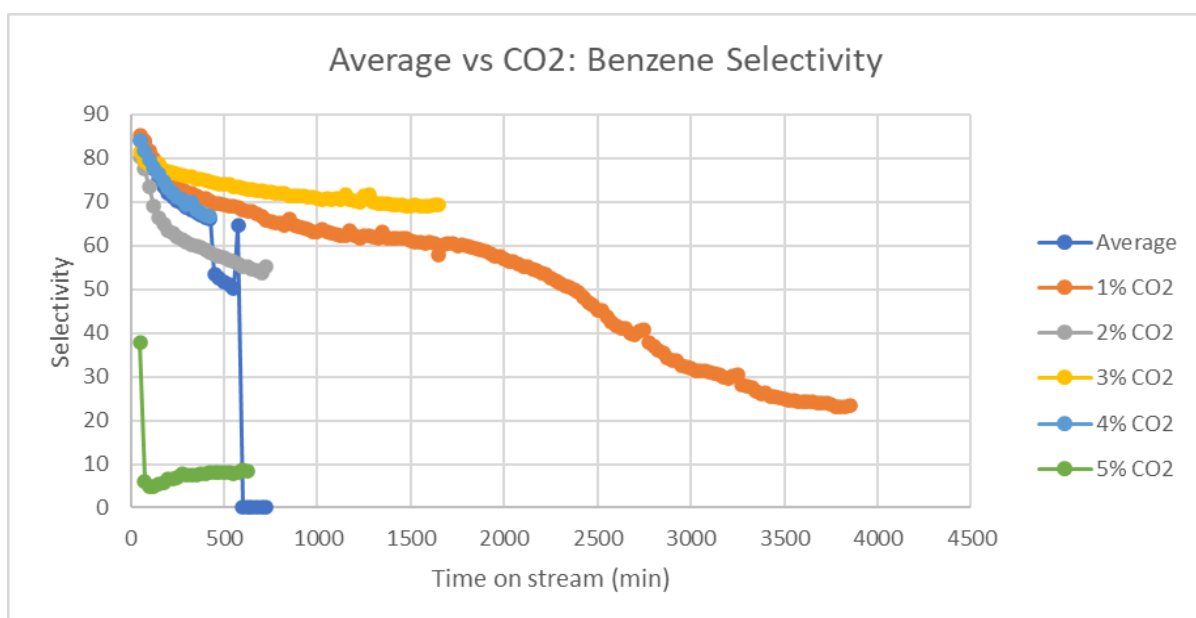
Figure 6: Average Baseline Benzene Selectivity vs Benzene Selectivity with CO_2

this in the next section, benzene is the intended final product. However, with methane conversion below 7% and benzene selectivity below 10%, there is no justifiable reason to use a 5 vol% gas addition of carbon dioxide. Looking at the first major result of 1 vol% carbon dioxide addition, it can be shown how carbon dioxide affects selectivity in the long term. After an initial decline from 85% benzene selectivity to 62% benzene selectivity (27% efficiency loss), the benzene selectivity stabilizes. This stabilization lasts for roughly 300-350 minutes (5-6 hours) before deactivation starts again. This gives insight on how carbon dioxide affects the reaction. This is explained later within the report. For now, it should be noted that carbon dioxide stabilizes benzene production after an initial efficiency loss. This can also be seen in a 3 vol% carbon dioxide addition. However, a 3 vol% carbon dioxide addition is the highest benzene selectivity compared to any other carbon dioxide additions. Initially, a 3 vol% addition has a lower benzene selectivity (~83% versus 85-88% on the others), however, once the reaction has passed 500 minutes on stream, the initial benzene selectivity drop is inconsequential.

3.1.4 C_2/C_7 Selectivity

As stated in the previous section, the goal of MDA is to increase the value of methane by reacting it into more valuable aromatics. One way to increase the value is by transforming it into ethane/ethene (C_2s). Fortunately, methane must transform into C_2s before reacting into benzene. *Figure 7* shows the selectivity to C_2s to all carbon dioxide additions. It should be noted that the 5 vol% carbon dioxide addition has very high C_2 selectivity. This is the final reason for 5 vol% being labelled the "catalyst death". The intended purpose of MDA is to raise the value of methane by transforming it into benzene. This makes methane much more valuable as benzene has numerous applications and can be used in many processes in the future. Other byproducts, such as ethane/ethene, also increase the value of methane, but not to the same degree as their applications are limited. Looking at *Figures 5-7*, it can be shown that any methane that has a 5 vol% gas addition that passes across a 2% Mo/HZSM-5 catalyst produces C_2 products. The amount of product that is created is far too low to be economically viable, as well as the product generated is a secondary product. Looking at a 1 vol% carbon dioxide addition, it is almost a perfect reflection of the benzene selectivity graph. This is also true for a 3 vol% carbon dioxide addition. However, C_2 is only one byproduct that can form. The other byproduct that can
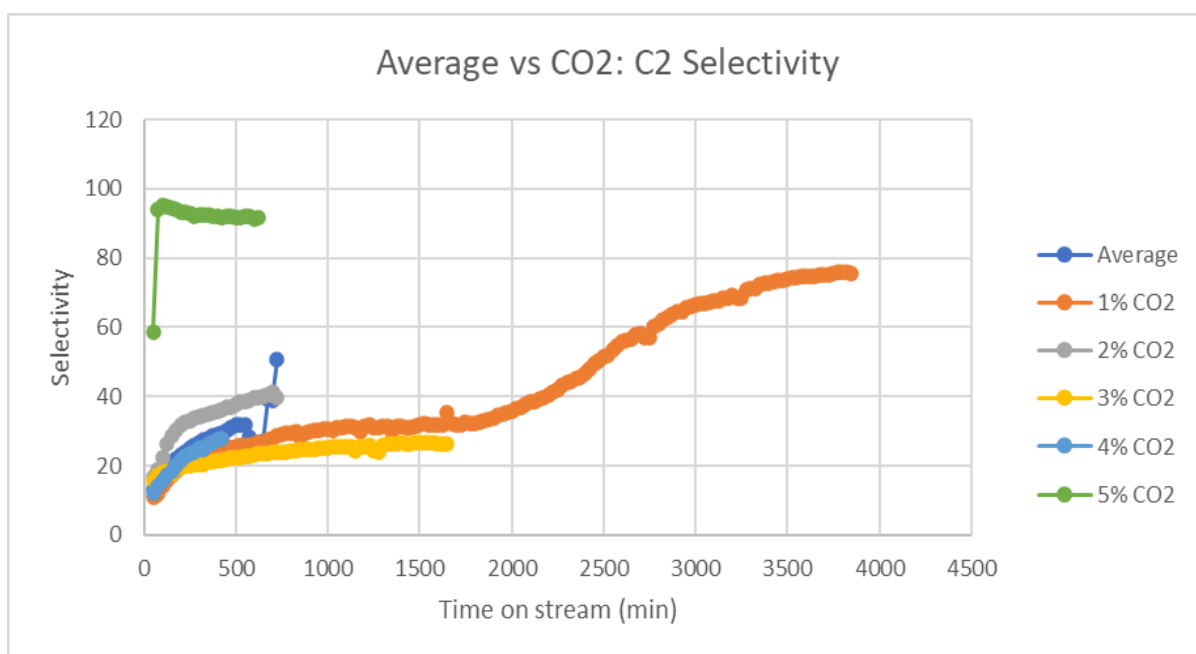

Figure 7: Average Baseline C$_2$ Selectivity vs C$_2$ Selectivity with CO_2

form is toluene (C_7s). Although toluene is a perfectly acceptable byproduct, which can be transformed into benzene much more readily, it is also the tipping point of the reaction. According to other reports, this reaction uses carbon radicals, carbons with free electrons, to react with one another to create larger hydrocarbons. As the reaction proceeds forward, however, the number of free radical sites increases. Due to the stability of benzene, it is very hard to create a radical and thus most methane transforms into benzene rather than PAHs. However, if benzene does react and forms toluene, or other benzene derivatives, the chances that it will transform into PAHs increases. Therefore, it is integral that the C_7 selectivity is as small as possible as that will limit how much benzene is transforming into PAHs. *Figure 8* shows that any addition of carbon dioxide, except for a 5 vol% addition, will inevitably increase the number of PAHs generated. This makes sense as, the amount of benzene increases, the number of PAHs should also increase as well. Looking at both 1 vol% & 3 vol% carbon dioxide addition, as the reaction proceeds forward, the amount of C_7s increases. In 1 vol% carbon dioxide addition, it can be shown that the amount of C_7 selectivity drops as the benzene selectivity drops. This is due to the catalyst deactivating limiting the amount of benzene being created. Therefore, as the benzene selectivity drops, so does the PAH selectivity.
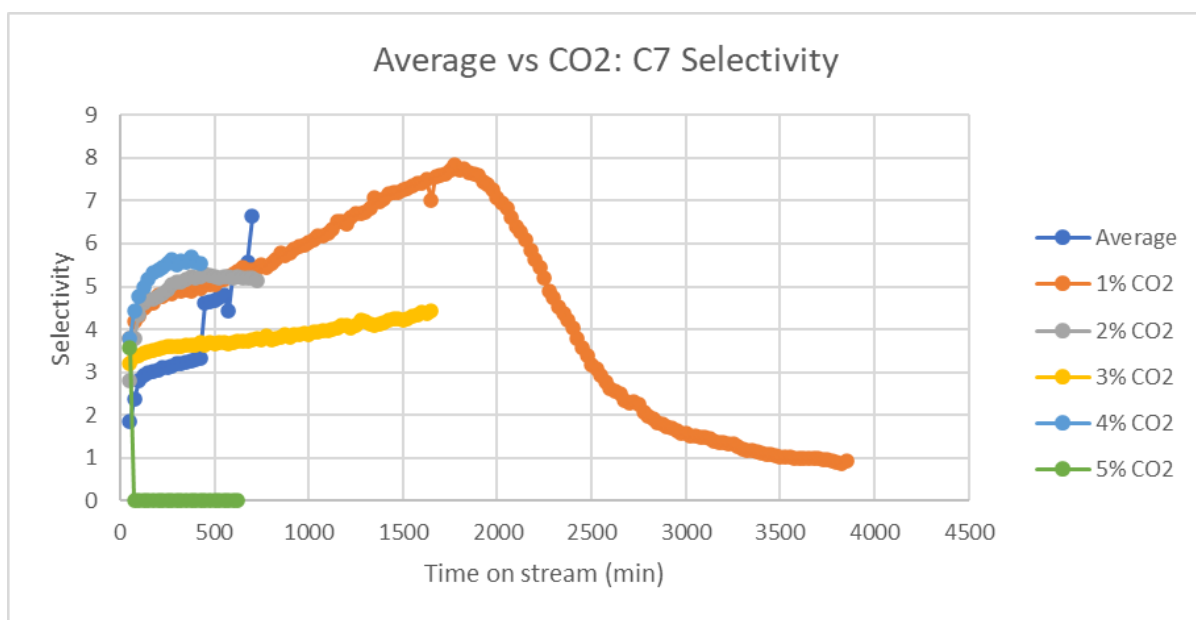

Figure 8: Average Baseline C_7 *Selectivity vs Baseline* C_7 *Selectivity with* CO_2

3.2 Temperature Programmed Desorption Test Results

3.2.1 Hydrogen TPD Results

        The reactionary pathway of MDA has been a long studied phenomenon. Because of the conditions in which the reaction is held in, it is difficult to determine what products form on the surface. One method that can be done, however, is temperature programmed desorption. This process heats up the catalyst and allows molecules to desorb. This is a good way to indicate bonding energy at certain temperatures for molecules. It can also be used as an indication of what types of molecules can be found on the catalyst's surface. A similar process was done in Ohnishi et al.'s report. The group used TPO instead of TPD. The main difference between the two processes is that TPO uses oxygen to help desorb higher bonding energy chemicals from the catalyst. TPD, on the other hand, uses a neutral gas to allow desorbing to occur. This first set of results used hydrogen gas.

        When initially testing the spent catalysts, the main chemicals that were tested for were based on the calibration of the gas chromatograph: benzene, toluene, ethane, ethene, and methane, as well as propane and water. Although water and propane were not calibrated into the gas chromatograph, they could indicate other phenomenon within the TPD results. Water was to determine when the zeolite started to deteriorate during TPD, and propane is a good indication of a reactionary pathway to benzene. Due to the amount of TPD results, they are located within Appendix A. The catalysts used, for the hydrogen trial, was a sample with no carbon dioxide addition and a sample with 1 vol% carbon dioxide addition. Looking at *Figures A 9-12*, both benzene and toluene did not desorb under hydrogen flow. A negative ionic current indication simply means that the mass spectrometer cannot find any ionic strength within the stream. Therefore, it can be theorized that any benzene and toluene that did not desorb during the time of the reaction became PAHs. This can be backed by *Figure A 6 & Figure A 8*. As the benzene selectivity decreases in the beginning, the C_7 selectivity increases, and therefore the PAH selectivity increases. Methane was also looked at to see how much reactant ended up on the surface of the catalyst. *Figure A 13 & Figure A 14* show that there is a weaker ionic current throughout the reaction. *Figure A 13* shows that with no

addition of carbon dioxide that there is a strong peak at $100°C$ with relatively strong peaks throughout the rest of the reaction. The same cannot be said though for *Figure A 14*. *Figure A 14* shows a strong peak towards the start of the reaction but has a fast decay before $100°C$ where it remains around the same ionic current. One theory of this increased ionic current is due to the increased amount of methanol on the catalysts surface. Looking at *Figure A 15 & 16*, a sample from the same catalyst was tested again, but methanol was tested for in the mass spectrometer. It should be noted that *Figures A 14 & 15* should be similar as it is the same sample. Looking at *Figures A 14-16*, the methane graphs are similar, but more importantly the methanol peak has a much higher ionic current than either methane graph. As explained later, a theory for why this occurs is due to carbon dioxide donating an oxygen to stabilize the methane molecule for the reaction. *Figures A 17-19*, show the ionic current of ethane. It can clearly be seen that there is a strong ionic current for the molecules throughout the TPD experiment. Much like methane though, the ionic current for ethane is very low for its selectivity. Therefore, ethane must be transforming into ethene. Looking at *Figures A 20 & 21*, the ionic currents of ethene is 1000 times greater than the ionic current of ethane. It can be concluded that ethene is more stable within the MDA reaction than ethane. *Figure A 22* shows the ethyne ionic current for 1 vol% carbon dioxide addition sample. Unlike ethene, ethyne does not increase the stability to ethene in the reaction. It can be theorized that ethene is a mandatory state for MDA to take place. *Figures A 23 & 24* show the propane peaks for a baseline catalyst sample and a 1 vol% catalyst sample. Both peaks are similar in nature having two strong peaks around $500°C$ and $700°C$. The largest difference between the two peaks is the gap in the $600°C$ range. With no carbon dioxide addition there is a strong peak, but with 1 vol% carbon dioxide addition there is a small peak detected. This brought up many questions as to why this happened. The water TPD results show why this was occurring. *Figures A 25 & 26* show the water peak desorption strength over the temperature range. It can be clearly seen in *Figure A 25* that with no carbon dioxide addition, there are water molecules desorbing at the $100°C$ temperature, i.e., the boiling point of water. This indicates that hydrogen is interfering with the zeolite and removing oxygens from the structure. The same can also be said with *Figure A 26*, however, there are secondary peaks because of the carbon dioxide addition. Because of this, the hydrogen addition can no longer

be used as it is poisoning the sample and creating false data. Therefore, the removing gas was changed to argon. Argon was chosen because of its nonreactive nature.

3.2.2 Argon TPD: Chemicals Tested

Because hydrogen has the potential to skew results, all previous results will need to be retested. However, due to the high stability of both benzene and toluene, they will not be retested. Hydrogen would have the greatest probability of removing any leftover benzene or toluene that was still on the catalyst's surface. Since the results showed no activity from either benzene nor toluene, it is safe to assume that any benzene and toluene react into PAHs. However, the same cannot be said for the other molecules tested. Since the mass spectrometer was able to detect all the other chemicals, they will need to be retested to ensure accuracy of the results. In addition, other chemicals were also added to help further understand the reactionary pathway of MDA. These chemicals were ethanol, propanol, propene, propyne, butane, butene, butyne, pentane, and hydrogen since it is no longer the removing agent in the system.

3.2.3 Argon TPD: Difference in Retested Chemicals

The TPD results for methane, methanol, ethane, ethene, propane, and water need to be retested. It is commonly known that the hydrogenation of alkenes and alcohols happens readily. Therefore, ensuring that this did not occur is critical. *Figures A 27 & 28* show the argon results for 1 vol% addition of carbon dioxide across two different samples. Comparing these results to *Figures A 14 & 15*, the ionic strength between the four graphs is similar. This means that the amount of methane poisoned by the hydrogen was minimal. This ensures that any conclusion drawn for at least methane is accurate so far. *Figures A 29 & 30* both show how methanol reacted under argon flow. Comparing these figures to *Figure A 16*, the ionic current of methanol is lower in the argon results. This is most likely due to the increased amount of hydrogen in the previous trial. It can be theorized that some oxygen remains on the catalyst's surface. This could then react with adsorbed methane to produce more methanol increasing its ionic strength. However, under argon flow, the amount of hydrogen within the system is limited; therefore, methanol production is unlikely. *Figures A 31 & 32*

show the results of ethane. These results indicate that the quantity of ethane on the catalyst is short lived rather than a constant flow as in *Figures A 17-19*. This is because ethene was hydrogenated leading to a false result. As stated previously, hydrogenation can occur on alkenes very readily, especially under high temperatures. This resulted in the constant flow of ethane rather than the sharp decline that *Figures A 31 & 32* depict. Although the ethane stream was artificially inflated, the conclusions drawn before are still accurate as the ionic current of ethene is still 1000 times stronger than ethane. This can be seen in *Figures A 33 & 34*. However, phenomenologically this changes how ethane reacts in MDA. According to the new results, ethane promptly turns into ethene while on the catalyst's surface instead of desorbing as ethane. Looking at *Figures A 35 & 36*, the propane results can be seen, and are much different from *Figures A 23 & 24*. *Figures A 23 & 24*, show that propane has multiple peaks at higher temperatures with a gap at around $600°C$. The only case where this wasn't true, was in the 0 vol% addition to carbon dioxide. However, in *Figures A 35 & 36*, the propane peaks have the same ionic current. Therefore, *Figures A 23 & 24* have also been poisoned by hydrogen. Shown later, this is due to propene and propyne being hydrogenated into propane. Truly, propane increases in ionic strength until $600 - 700 °C$ when it finally desorbs off the catalyst's surface. This can be seen in *Figures A 23 & 24*, but because of the poisoning of the sample, the peaks help define the points in which propene and propyne are hydrogenated. Finally, *Figures A 37 & 38* show the new water peaks within argon flow. Comparing these figures to *Figure A 25 & 26*, the argon trial depicts water leaving the system, while the hydrogen trial shows water being generated within the system. This can mean that the catalyst's zeolite remains intact throughout the entire process. This can also show that oxygen is minimized on the catalyst and reacts readily on the catalyst.

3.2.4 Argon TPD: New Chemicals

Ethanol, propanol, butane, butene, butyne, pentane, hydrogen, propene, and propyne are good indicators how MDA transforms into benzene. Finding the presence of ethanol or propanol can depict that longer hydrocarbon chains need a leaving group to transform into benzene. *Figures A 39-44* show the ethanol and propanol results for 1 vol% to 3 vol% addition of carbon dioxide. Across all the different samples, both ethanol and propanol do

not show up within the mass spectrometer except for a single point at the start of the experiment. This can either mean that ethanol and propanol do exist in the reaction but are not adsorbing to the catalyst/ are consumed almost immediately, or that this is just some noise within the reaction. Based on later results, i.e., propyne, it is most likely that if either alcohol exists, they are transformed into ethene or propyne. *Figures A 45-47* show whether butane and its derivatives exist in the reaction. Using 3 vol% carbon dioxide addition as the model, the butane family does not exist. 3 vol% carbon dioxide was used because it was the sample that generated the most benzene, and thus would have the best chance of finding these chemicals. The same trend is found in other vol% of carbon dioxide additions, except for a few points at the very beginning. This follows the same trend as ethanol and propanol. However, looking at *Figure A 48*, pentane shows almost no ionic current on the catalyst. It was then theorized that if pentane does not exist, then butane most likely does not exist either. It was theorized that these small ionic strength peaks, such as the singular points at the beginning of the TPD trial, are insignificant to the overall result. Therefore, given the figures, it can be theorized that when the MDA reaction occurs that it must happen very rapidly such that hydrocarbons above propane do not exist, or that hydrocarbons below butane must be the primary reactants towards benzene. This leads to the propane derivatives. As seen in earlier figures, propane was among the higher ionic current in the reaction, comparable to methane. However, *Figures A 49-51* show propyne as a dominant reactant on the catalyst's surface. Although propene does exist, as shown in *Figures A 52-54*, propene does not have a comparable ionic current to propyne. The only chemical with a similar ionic current is ethene and argon, the removing gas. Looking at *Figure A 55*, the TPD result for argon can be seen. This means that the amount of propyne located on the catalyst's surface is comparable to the amount of argon flowing into the mass spectrometer. It should also be noted that in *Figures A 56-58* there is little hydrogen off gas from the catalyst surface. This means that is either used or expelled from the reaction.

3.3 Analysis of Data

3.3.1 Transformation to Benzene

  The MDA reaction is not very well understood, and with each research that comes out a new hypothesis for the reaction is considered. With the TPD results, a clearer picture of how the reaction progresses can be theorized. Methane reacts transforming itself into ethene and eventually to propyne. This can be explained by Colket & Seery's work at the United Technologies Research Center (UTRC).[21] Their work demonstrated how methane can react and transform into toluene through pyrolysis at high reaction temperatures ($\sim 1100 K$ to $2000 K$). With this they showed that carbon becomes radical and transforms into more stable configurations.[21] With their work, methane and ethane radicalize to transform into the next stable hydrocarbon, propane. The catalyst can then remove hydrogens from the propane to create propyne. The reason for the propyne creation is mesitylene. Mesitylene is the common name of 1,3,5 methylbenzene. Because a zeolite is used to limit the size of reactions, it can be theorized that the supporting structure cleaves off the methyl groups creating methane and benzene. The role of carbon dioxide within MDA occurs at two different stages. Firstly, carbon dioxide stabilizes the reaction by reacting with the catalyst and donating oxygens to the methane. It can be seen in *Figures A 29 & 30* that methanol is more abundant than methane. The oxygen must be donated from a place other than the zeolite as seen in the water TPD results, *Figures A 37 & 38*. Therefore, the only other chemical with oxygen is carbon dioxide. This was also shown in Vollmer et al.'s experiment on carbon monoxide tracing.[20] Using the C^{13} isotope in carbon monoxide, they were able to trace the reaction and show that the C^{13} does end up within the benzene ring. This means the oxygens located on carbon dioxide are donated to the catalyst and are used in subsequent reactions. As stated, radical carbon is very unstable, this leads to the reaction happening very quickly and spontaneously. However, adding oxygen to the catalyst allows methane to gain a leaving group in the form of an alcohol. This can be done when both methane and oxygen are adsorbed onto the catalyst. From there, they bond with one another, and some hydrogen hydrogenates the oxygen to create methanol. The second use of carbon dioxide is theoretical. Using *Figure 5*, the conversion of each carbon dioxide experiment can be seen. Of all the different carbon dioxide additions, only 3 vol% of carbon dioxide

addition maximizes benzene selectivity. Comparing the TPD results of 3 vol% to the other volume percentages shows very little to no difference except for propyne. This can be easily explained as 3 vol% maximizes benzene production. However, across all the different results, 3 vol% of carbon dioxide was consistently performing the best. If the difference between each addition cannot be measured by TPD, then carbon dioxide must be altering the reaction in another way.

3.3.2 Carbon Dioxide: Arc Quenching

A known property within carbon dioxide is the ability to "arc quench".[22] Arc quenching is simply the phenomenon that a gaseous chemical reduces the number of free electrons within a given area at such a rate that electrical arcing is not possible. This can be seen by chemicals such as sulfur hexafluoride. The main use of these chemicals is to reduce the number of sparks generated in places where a large electrical current is flowing. Sulfur hexafluoride is one of the strongest arc quenchers and carbon dioxide, comparatively, is not as strong but still shows the same property.[22] The reason this is important is due to the radicalization of hydrocarbons within the reaction. As stated earlier, Colket and Seery's experiments were on the pyrolysis of methane to toluene and showing the radicalization of carbons.[21] Radicalization of any atom is simply an unpaired electron. Arcs/sparks are just a group of free electrons flowing. If carbon dioxide can suppress free electron flow within an arc, then the same can be said in a reaction. This is the main reason why carbon dioxide can control the reaction to this degree. Then why is it most prominent at this point? According to Yokoi et al's experiment in Aichi Institute of Technology, Japan, there is a formula that dictates the behavior of electrons within the gas.[23] *Equation 2*, shows how electrons will act within carbon dioxide:

$$\frac{\delta f}{\delta t} + v \times \nabla f - \frac{e}{m_e} E \times \nabla_v f = C(f) \qquad \textit{Equation 2}$$

where e, m_e, f, v and C are elementary charge, mass of electron, electron energy distribution function (EEDF), draft velocity of electron and the rate of change in f due to collision, respectively. The two most important variables are f & δt as they represent the energy of the electron and the collision rate of the electron. It can be theorized that as the volume

percentage of carbon dioxide increases, the collision rate increases and thus the energy of the electron depletes. When the vol% of carbon dioxide is too low, the amount of energy within the electron is still too high and thus the properties of MDA are unaffected. However, at a 3 vol% addition, the amount of carbon dioxide within the stream is high enough to start reducing the electron energy such that it is no longer thermodynamically favorable to transform into PAHs and instead remains as benzene. This can be seen in *Figure 8*, C_7 selectivity. As benzene selectivity decreases, the C_7 selectivity does not increase at the same rate, instead the C_2 selectivity increases at a much faster rate. This should not occur on a fundamental level because PAHs are more stable than benzene. Therefore, if benzene production drops/increase, so should PAHs at a similar rate. With a 3 vol% carbon dioxide addition, this is not the case. However, too much carbon dioxide has the exact opposite effect. As seen in the same figure, as more carbon dioxide is added into the stream, the number of PAHs decreases, but so does the amount of benzene. This can mean that there is a point in which the electron energy is slowed down too far, and the next stable hydrocarbon is not an aromatic, but instead propyne, ethene, or methane.

CHAPTER 4

Conclusion

4.1 Summary

Within this paper is the MDA work with carbon dioxide. The paper set out to study more in depth the relation carbon dioxide has with MDA and the mechanism in which MDA proceeds in. The work started with a baseline testing of a 2 wt% Mo catalyst with a HZSM-5 zeolite supporting structure. Carbon dioxide was then added to each subsequent test starting at 1 vol% and ending at 5 vol% with an increment of 1% per new trial. The catalyst has the potential to last over 60 hours of continuous experimentation with no regeneration when the inlet feed stream contained carbon dioxide at 1 vol%. This increases the lifetime of the catalyst over 700% using a 7 hour catalyst lifetime as the baseline. However, the effective catalyst lifetime increase is just over 1500 minutes (25 hours), to keep methane conversion above 10% and selectivity to benzene over 60%, which is 250% increase to its lifetime. The most notable result was that of 3 vol% addition of carbon dioxide to the gas stream, where conversion stabilized above 15% for over 1500 minutes and keeping selectivity to benzene around 70% for the same duration. The TPD results allowed this study to theorize that carbon dioxide transforms methane into methanol so that the reaction may proceed quicker. It was also shown that propyne is the dominant species on the catalysts surface. It was theorized that MDA reacts propyne into mesitylene and the methyl groups are then cleaved. It was also shown that carbon dioxide has arc quenching capabilities that can be used to ensure the reaction is stabilized and leads to benzene production. However, it was also shown that it can have the exact opposite effect and create more non-aromatic products rather than aromatic products.

4.2 Future Work

For future work, there are two main areas that need to be tested. The most important area is determining if mesitylene is being created. This can be achieved through nuclear magnetic resonance (NMR), more specifically magic angle spinning (MAS) NMR. What

MAS-NMR can tell is the bond lengths between the hydrogen and carbon on the benzene ring. If mesitylene is being produced, then the hydrogen on the benzene ring will have a different bond length than the hydrogens on the methyl groups on the benzene. This difference in bond length can determine what is being produced. However, this can be a problem as it must be done in-situ as mesitylene should not last long within the zeolite structure. With this type of data, the mechanism of MDA can be understood further. Another important area is verifying carbon dioxide's conversion within the gas stream. This will help ensure that the amount of methane going through and reacting is the posted value. It will also ensure that the selectivities to benzene are also accurate as well. Finally, examining the PAH content on the catalyst should be done to see how resistant the catalyst is to coking. This can be done using thermogravimetric analysis.

Appendix A: Temperature Programmed Desorption Figures
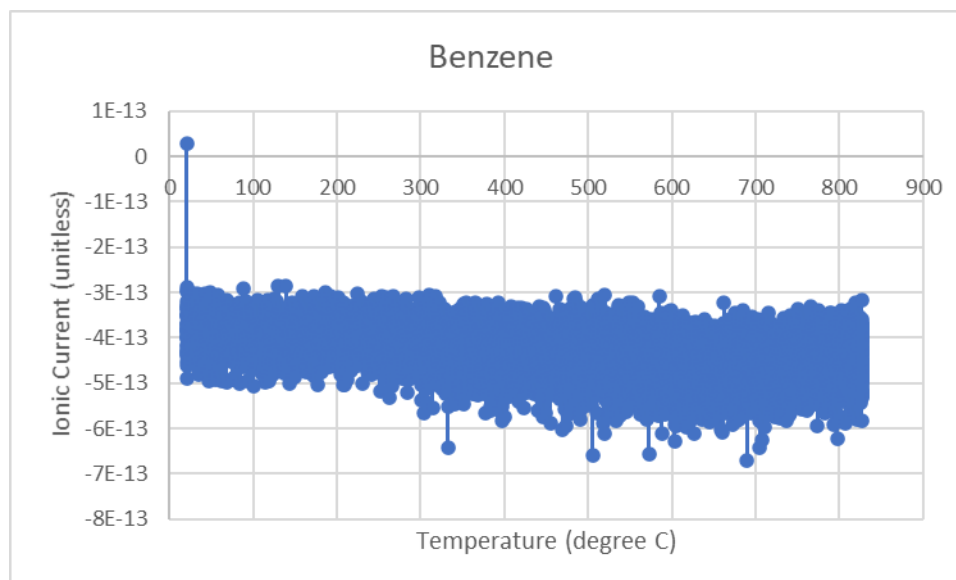
Figure A 9: 0% CO_2 Benzene TPD (sample 6-23 result)
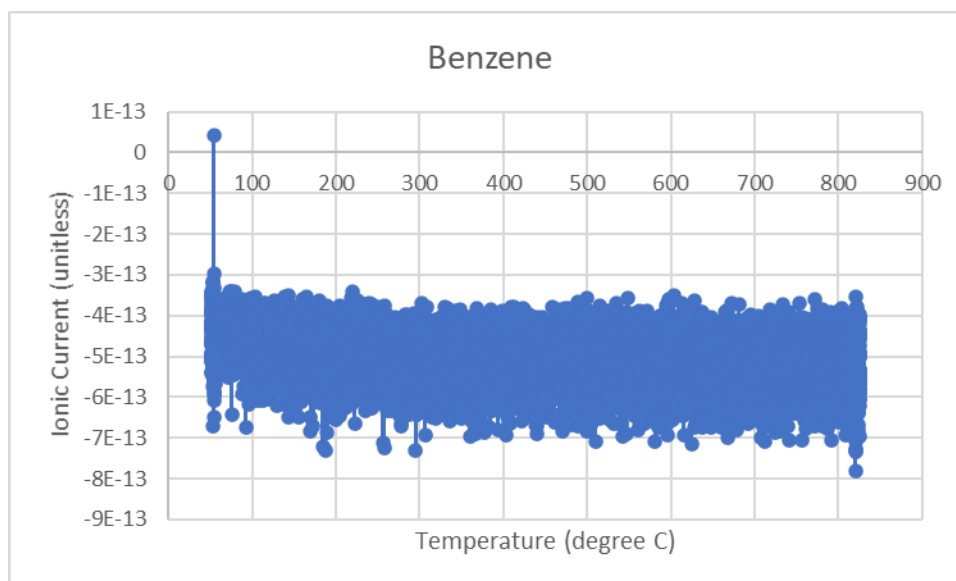
Figure A 10: 1% CO_2 Benzene 1st TPD (sample 6-26 result)
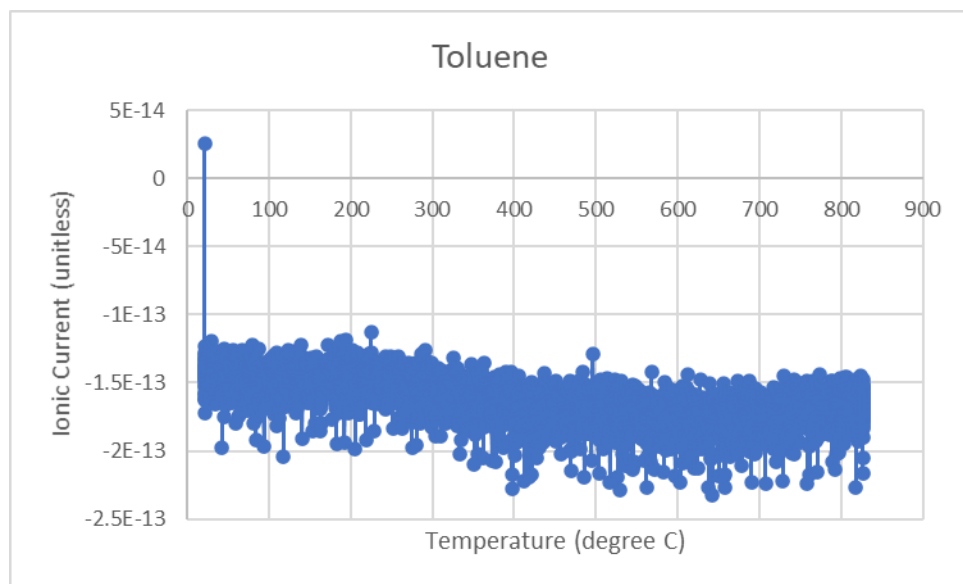
Figure A 11: 0% CO_2 Toluene TPD (sample 6-23 result)
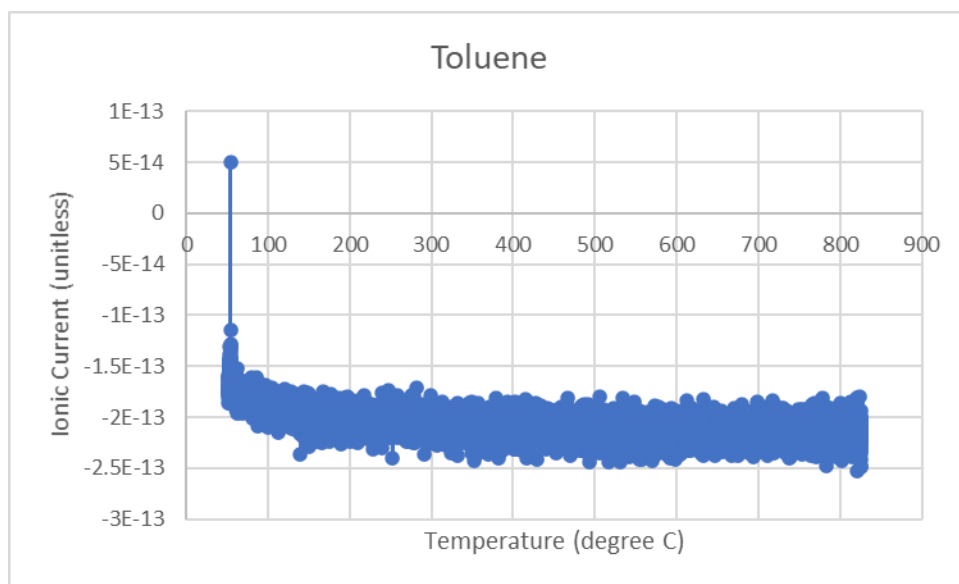
Figure A 12: 1% CO_2 Toluene 1st TPD (sample 6-26 result)
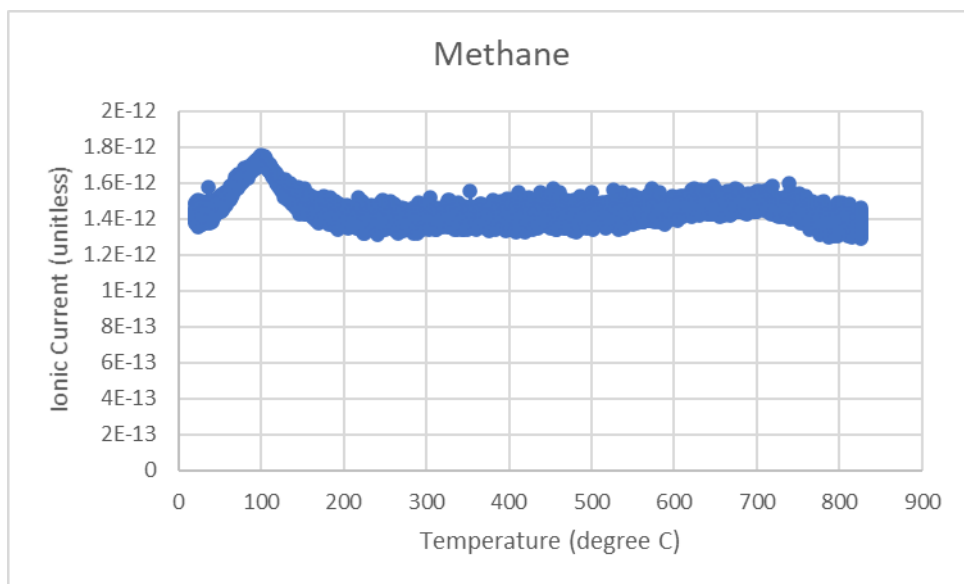
Figure A 13: 0% CO_2 Methane TPD (sample 6-23 result)
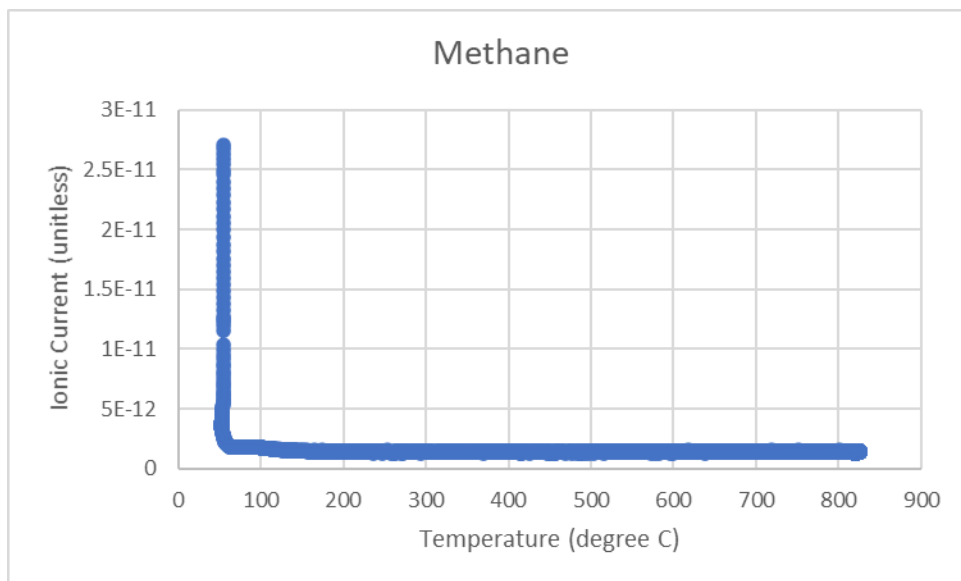
Figure A 14: 1% CO_2 Methane 1st TPD (sample 6-26 result)
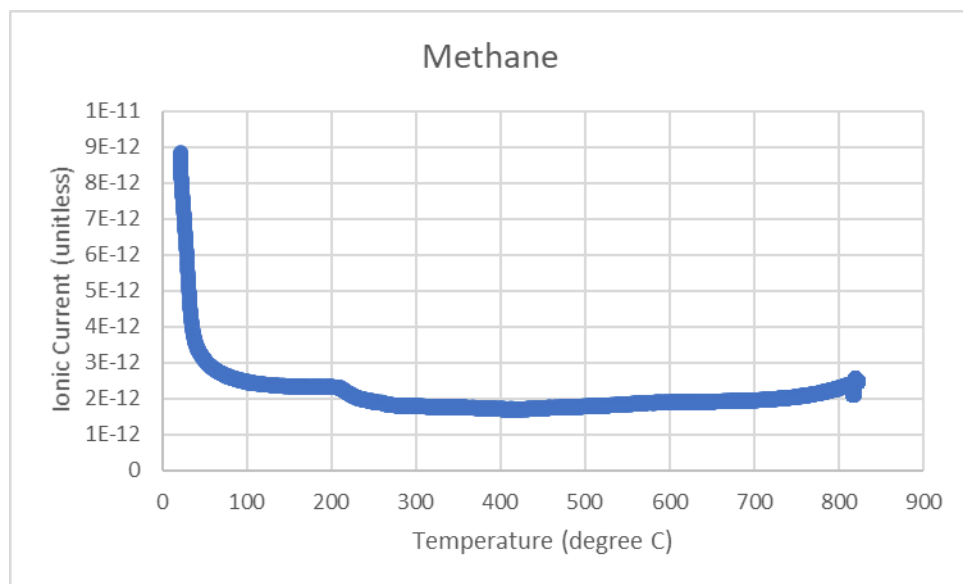
Figure A 15: 1% CO_2 Methane 2nd TPD (sample 6-26 result)
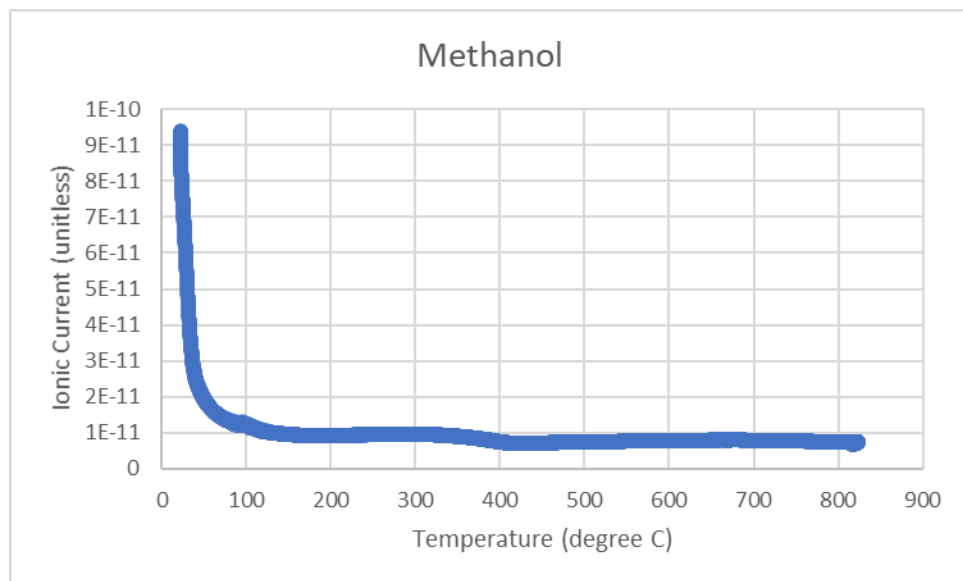
Figure A 16: 1% CO_2 Methanol 2nd TPD (sample 6-26 result)
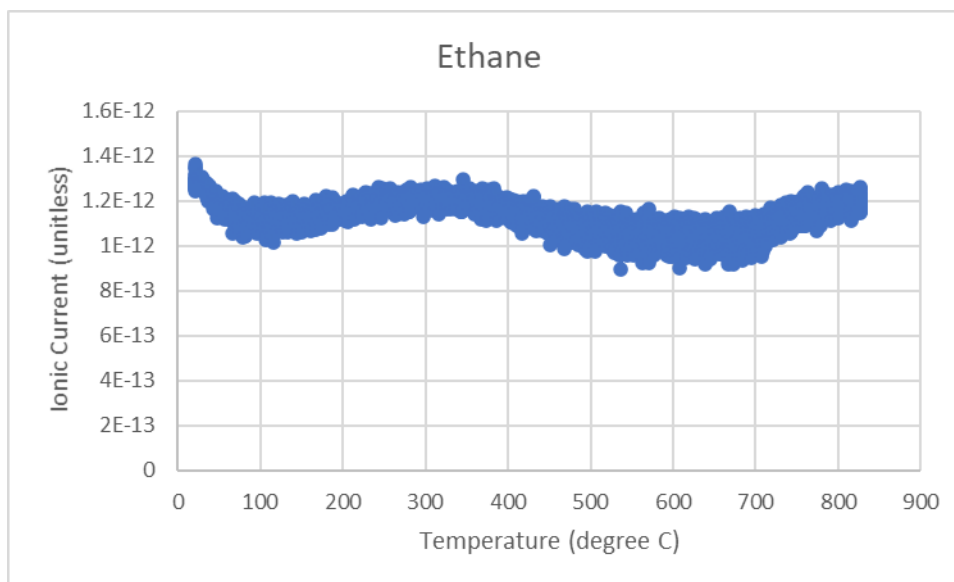
Figure A 17: 0% CO_2 Ethane TPD (sample 6-23 result)
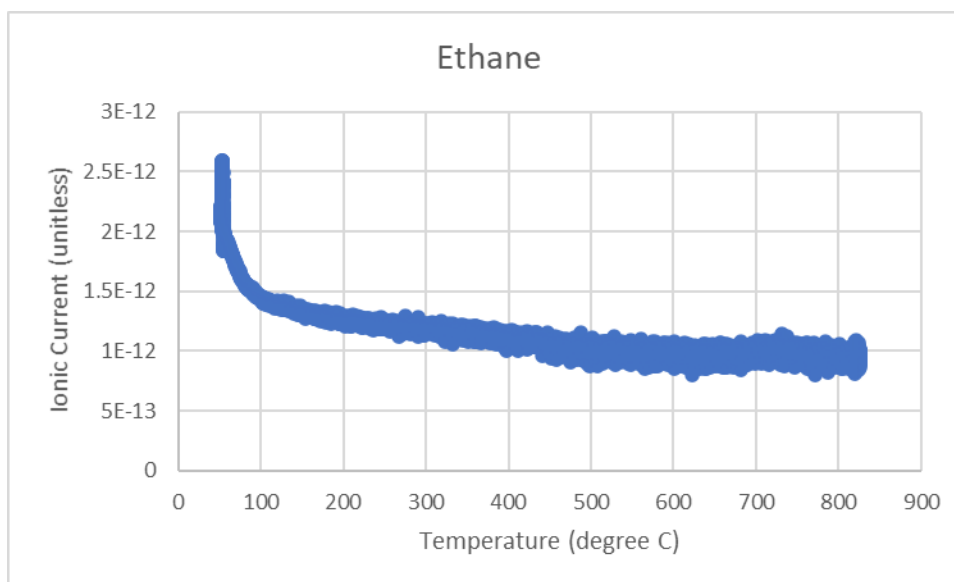
Figure A 18: 1% CO_2 Ethane 1st TPD (sample 6-26 result)
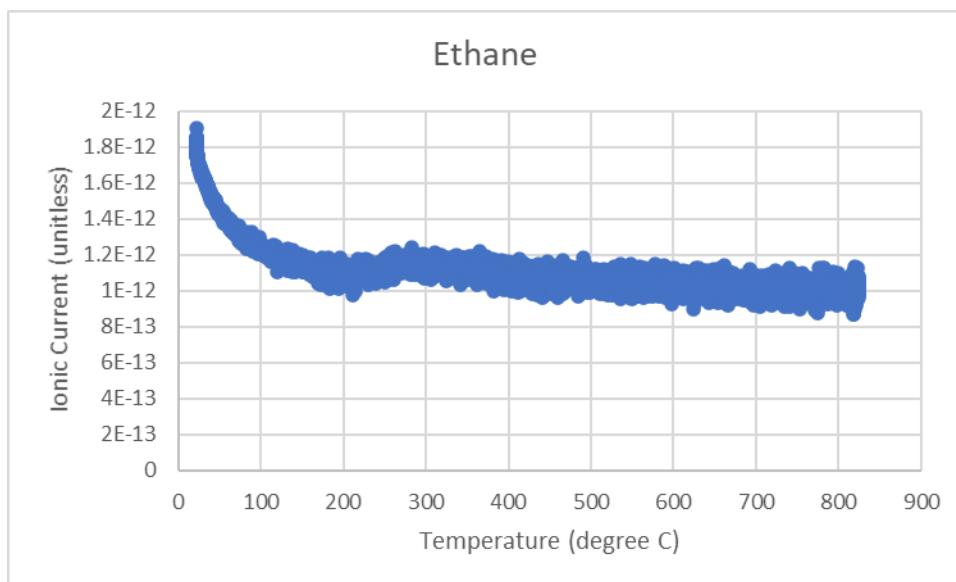
Figure A 19: 1% CO_2 Ethane 2nd TPD (sample 6-26 result)
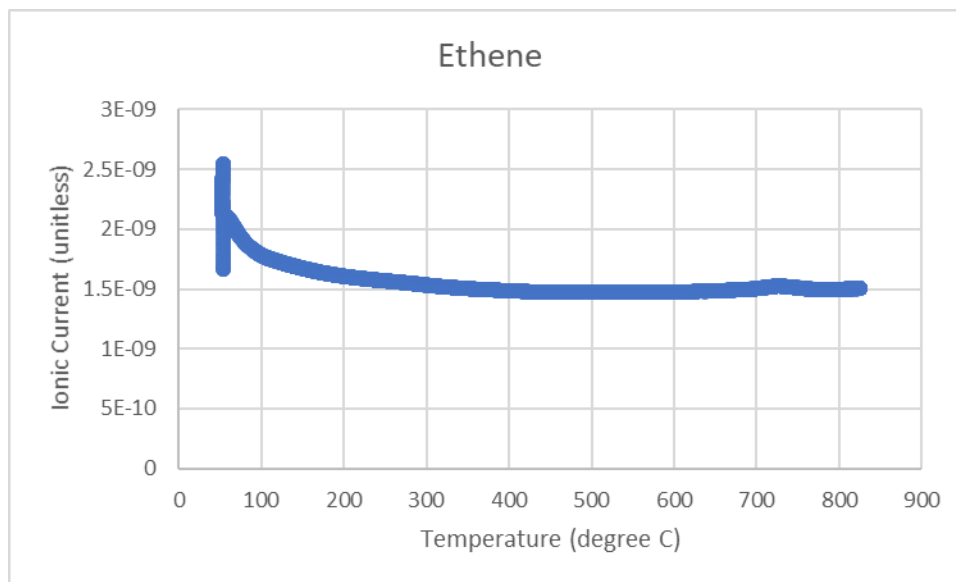
Figure A 20: 1% CO_2 Ethene 1st TPD (sample 6-26 result)
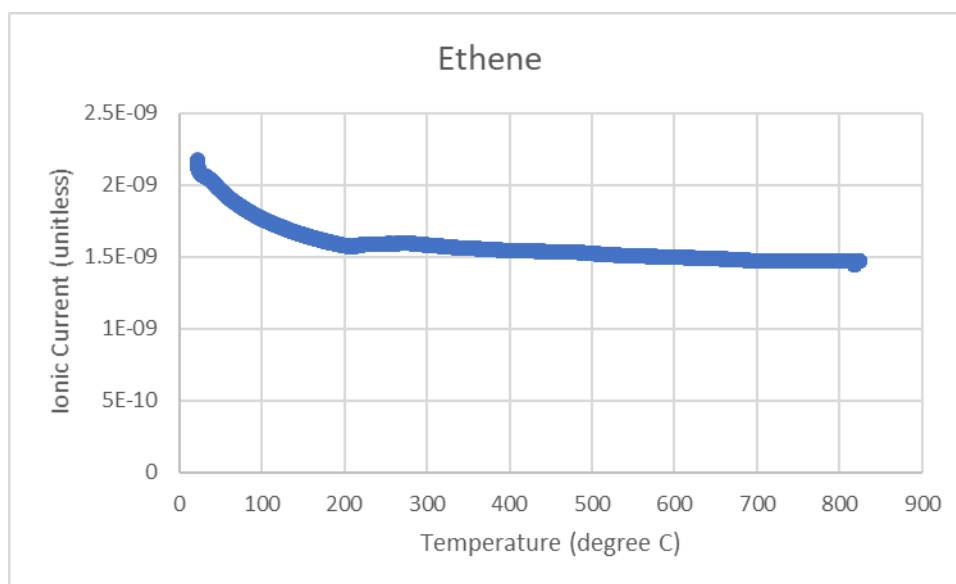
Figure A 21: 1% CO_2 Ethene 2nd TPD (sample 6-26 result)
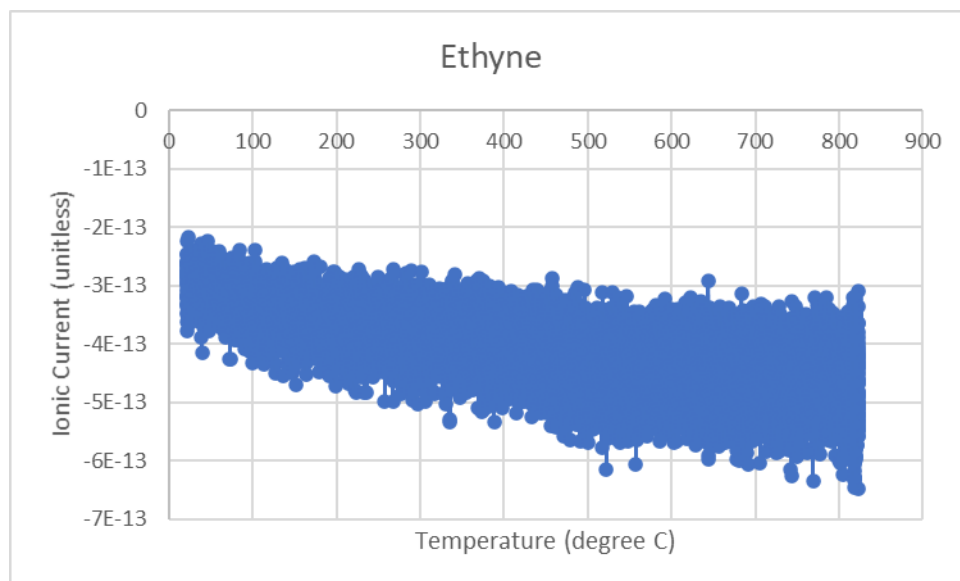
Figure A 22: 1% CO_2 Ethyne 2nd TPD (sample 6-26 result)
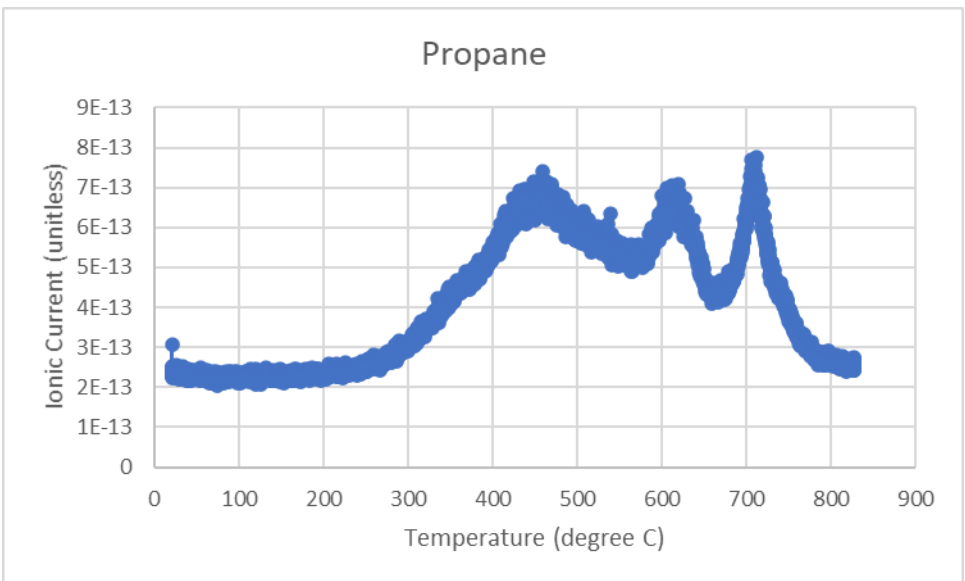
Figure A 23: 0% CO_2 Propane TPD (sample 6-23 result)
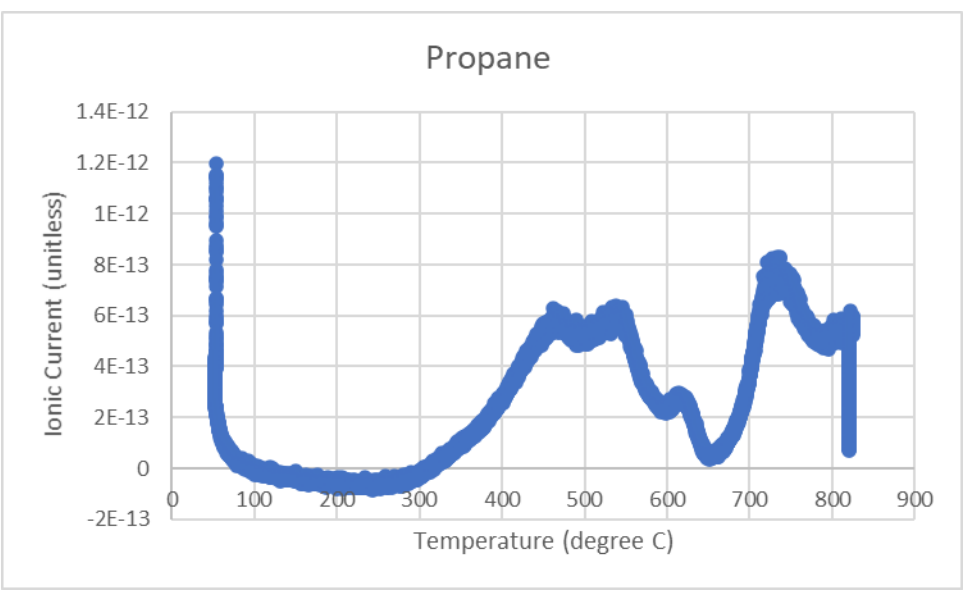
Figure A 24: 1% CO_2 Propane 1st TPD (sample 6-26 result)
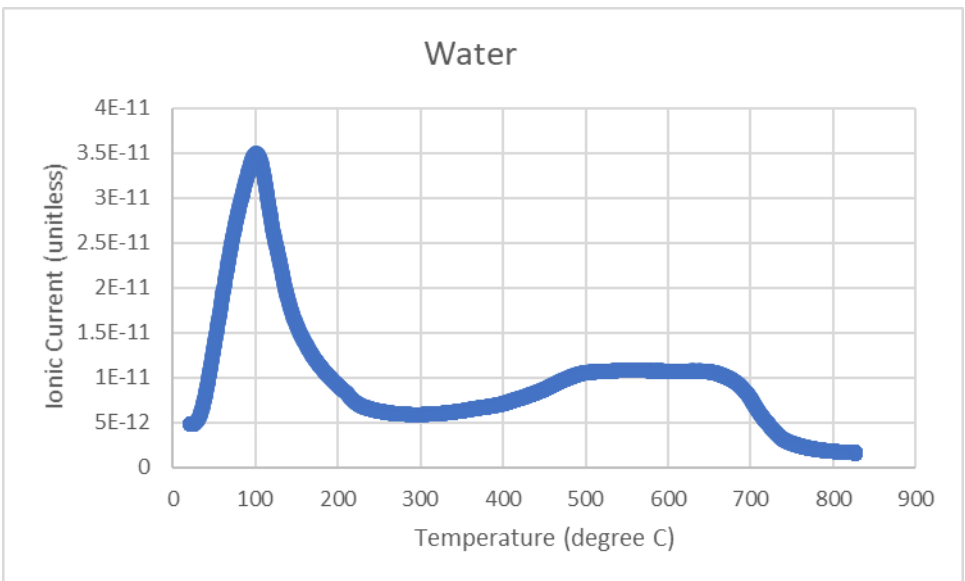
Figure A 25: 0% CO_2 Water TPD (sample 6-23 result)
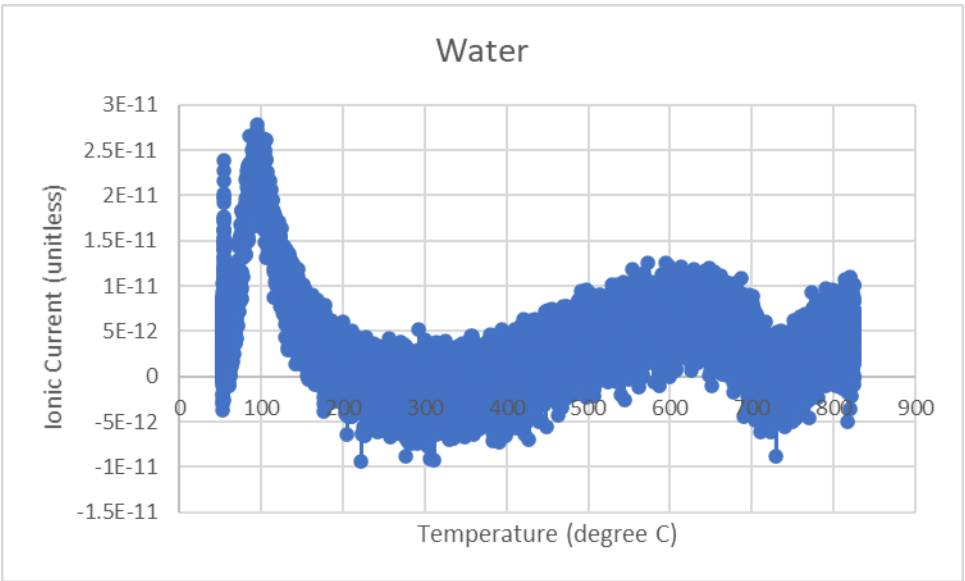
Figure A 26: 1% CO_2 Water 1st TPD (sample 6-26 result)
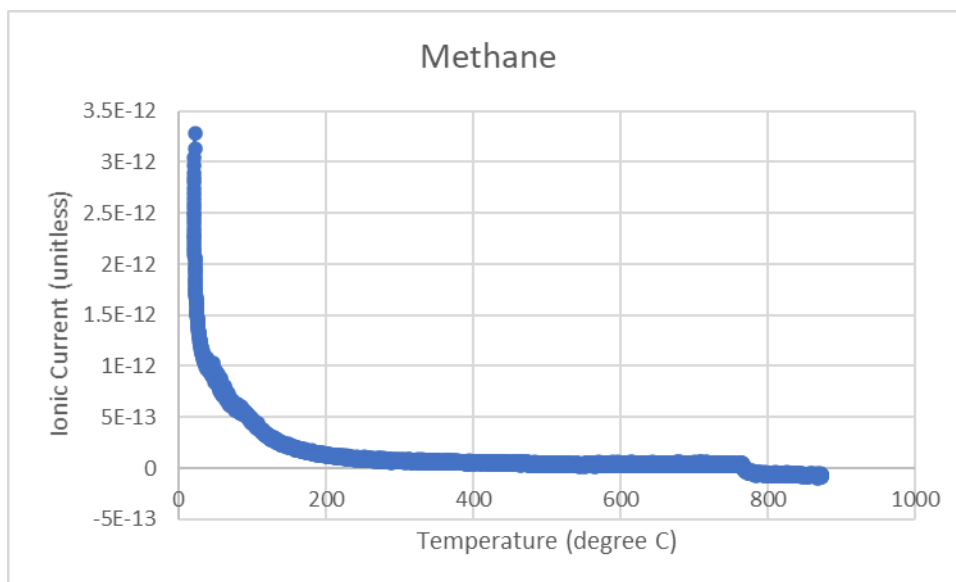
Figure A 27: 1% CO_2 Methane TPD (sample 6-29 result)
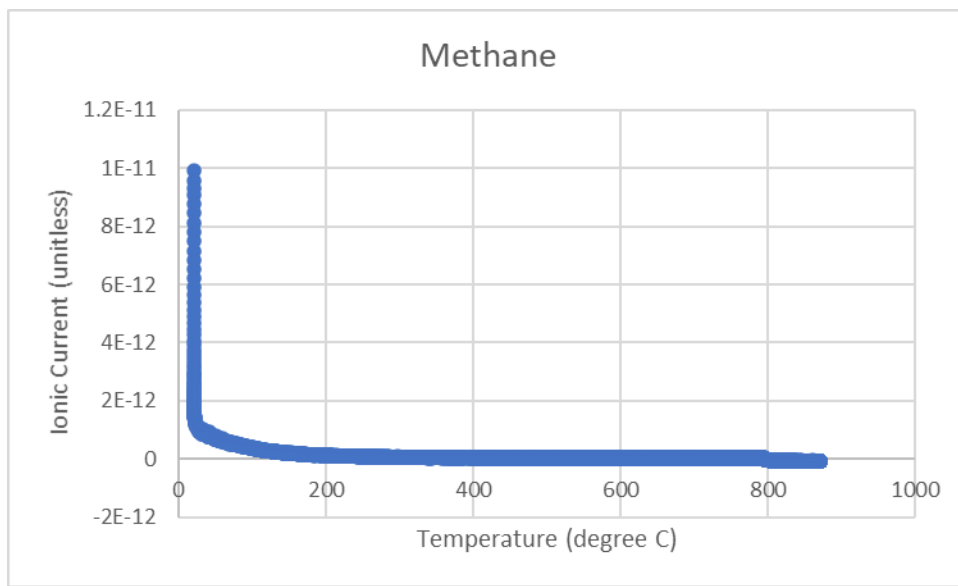
Figure A 28: 1% CO_2 Methane TPD (sample 7-07 result)
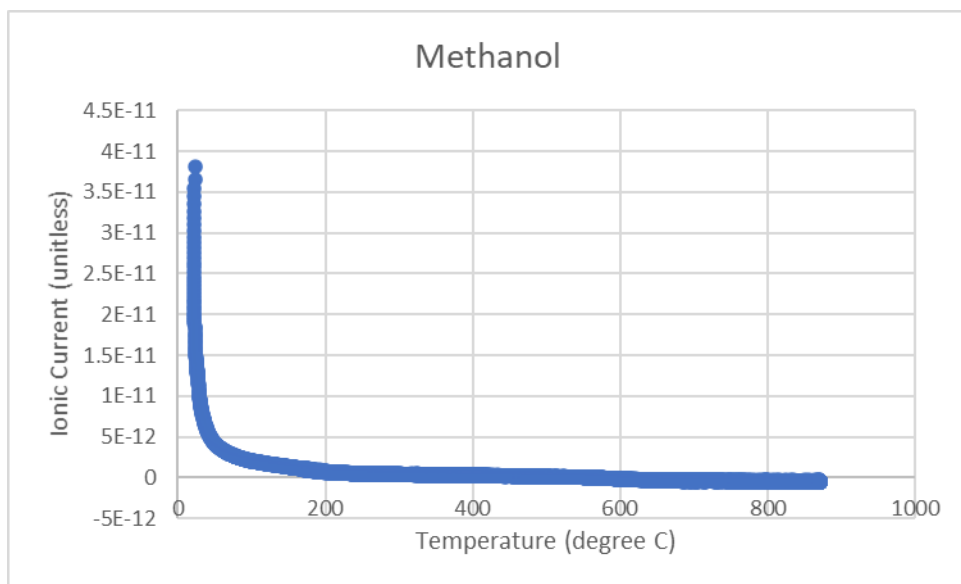
Figure A 29: 1% CO_2 Methanol TPD (sample 6-29 result)
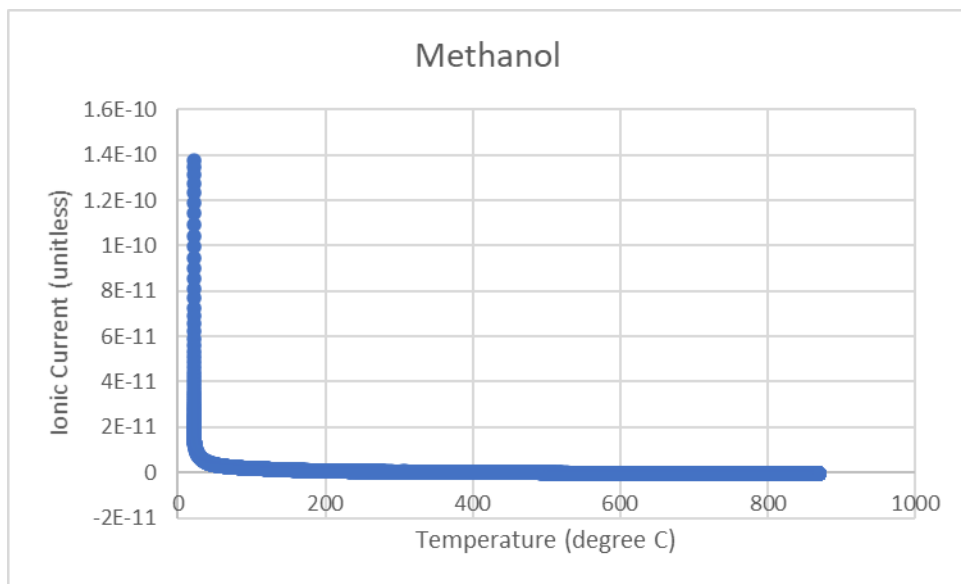
Figure A 30: 1% CO_2 Methanol TPD (sample 7-07 result)
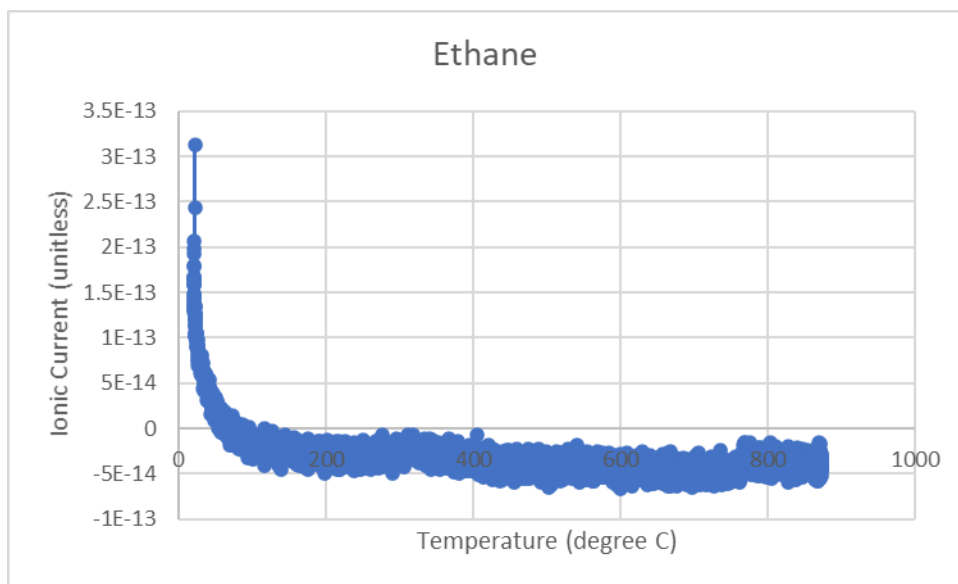
Figure A 31: 1% CO_2 Ethane TPD (sample 6-29 result)
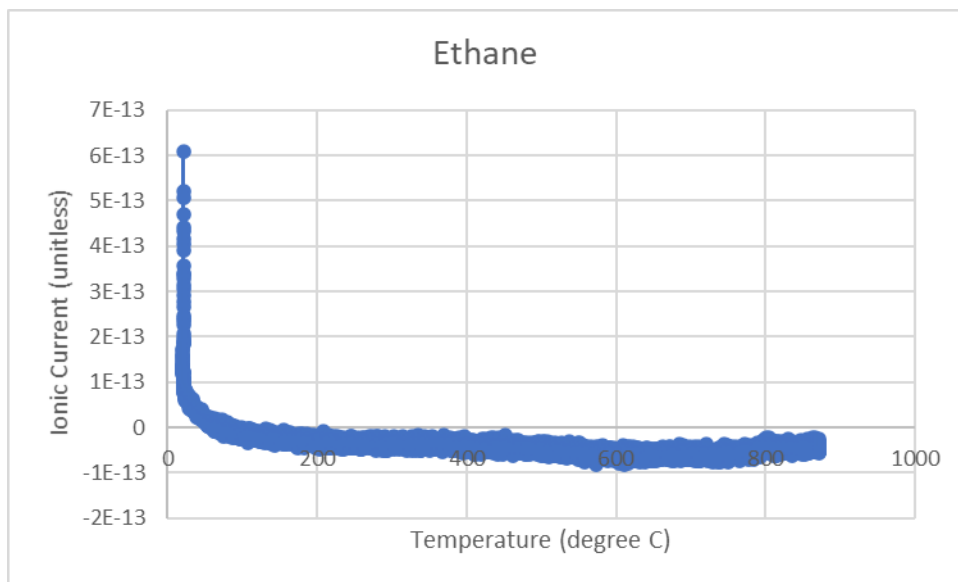
Figure A 32: 1% CO_2 Ethane TPD (sample 7-07 result)
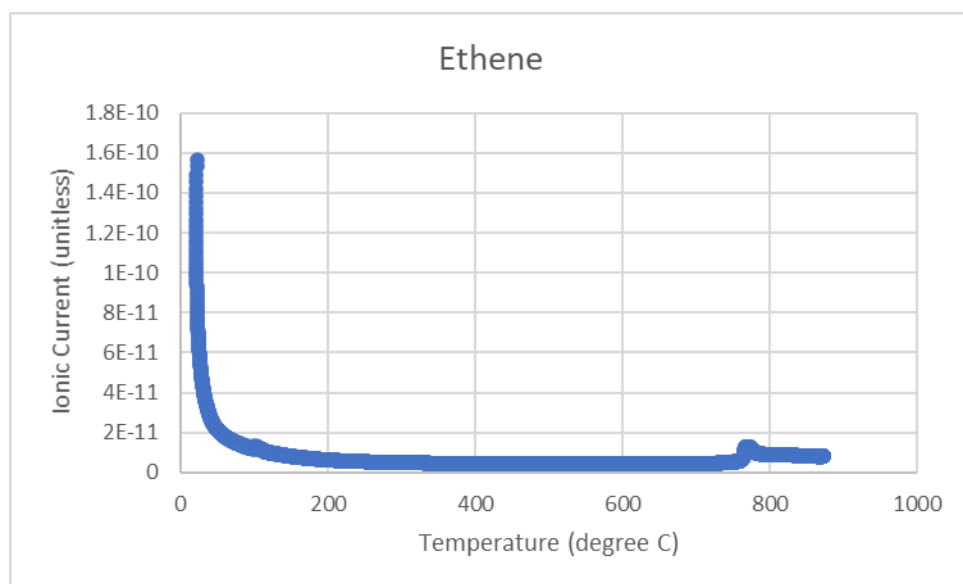
Figure A 33: 1% CO_2 Ethene TPD (sample 6-29 result)
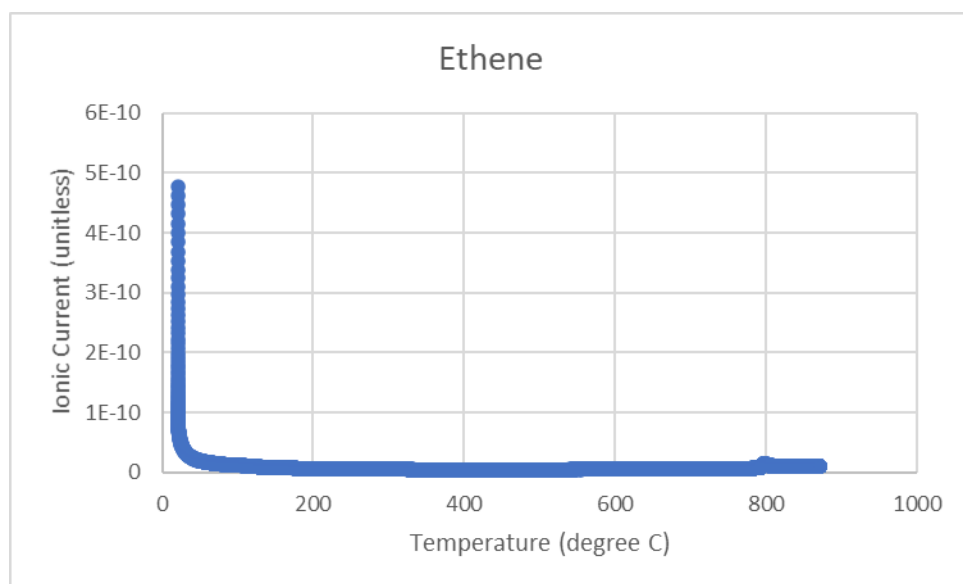
Figure A 34: 1% CO_2 Ethene TPD (sample 7-07 result)
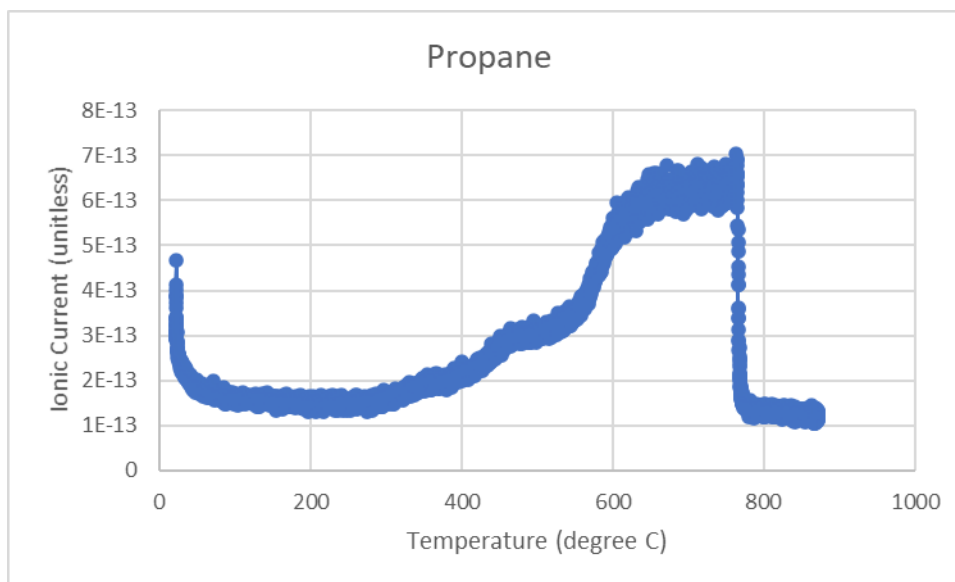
Figure A 35: 1% CO_2 Propane TPD (sample 6-29 result)
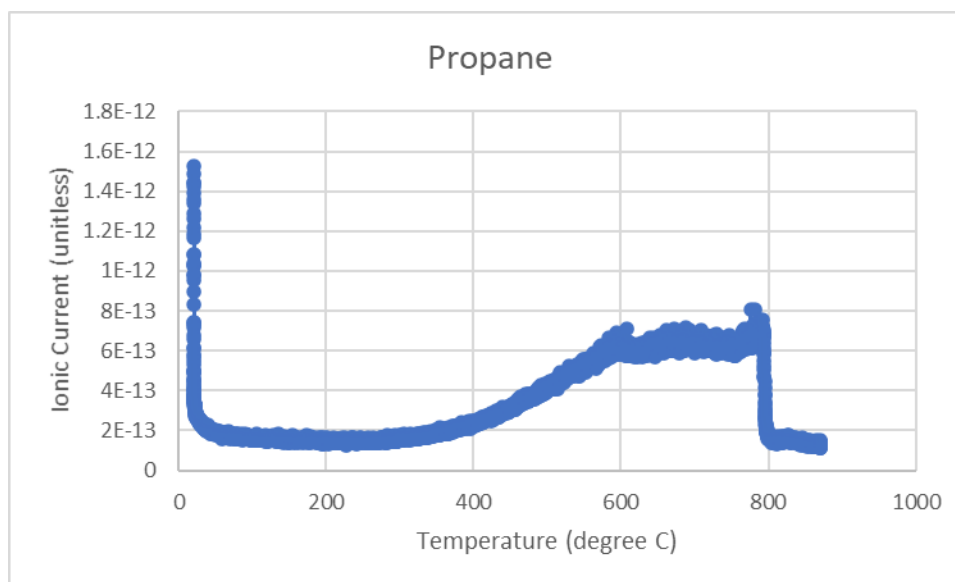
Figure A 36: 1% CO_2 Propane TPD (sample 7-07 result)
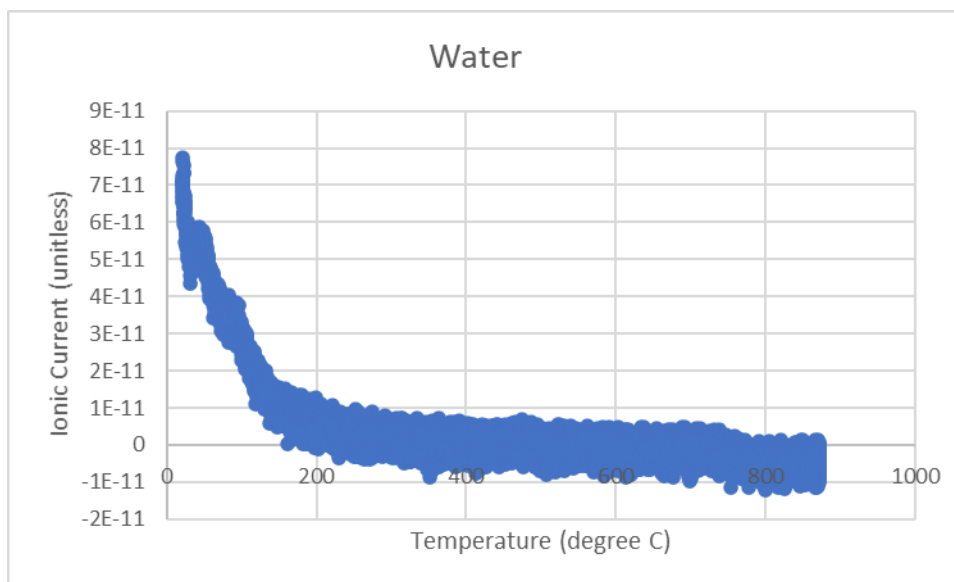
Figure A 37: 1% CO_2 Water TPD (sample 6-29 result)
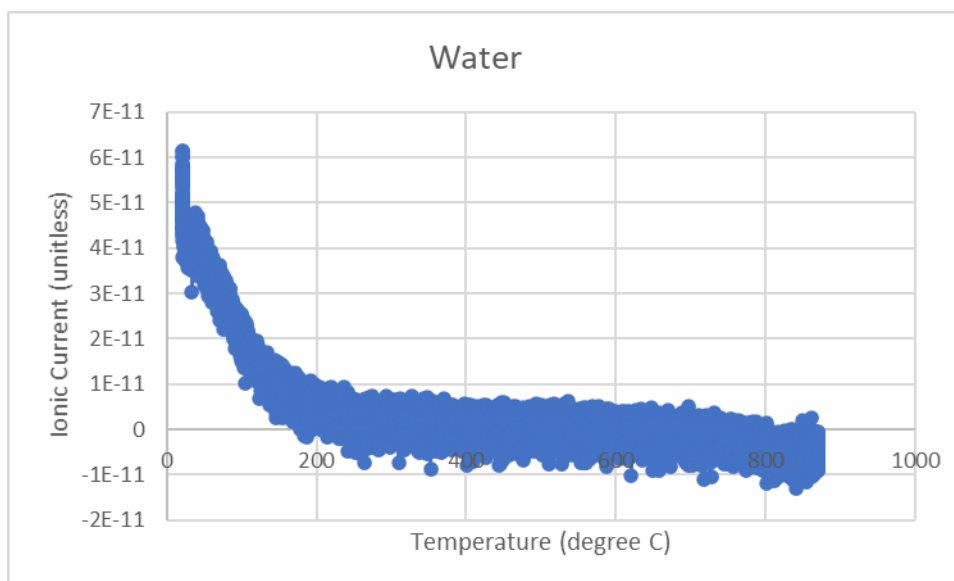
Figure A 38: 1% CO_2 Water TPD (sample 6-29 result)
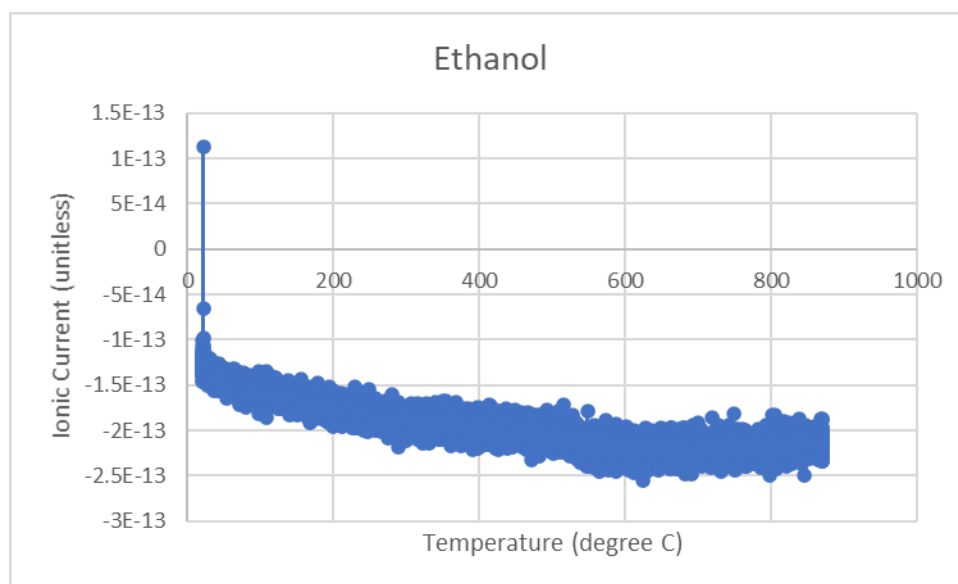
Figure A 39: 1% CO_2 Ethanol TPD (sample 7-07 result)
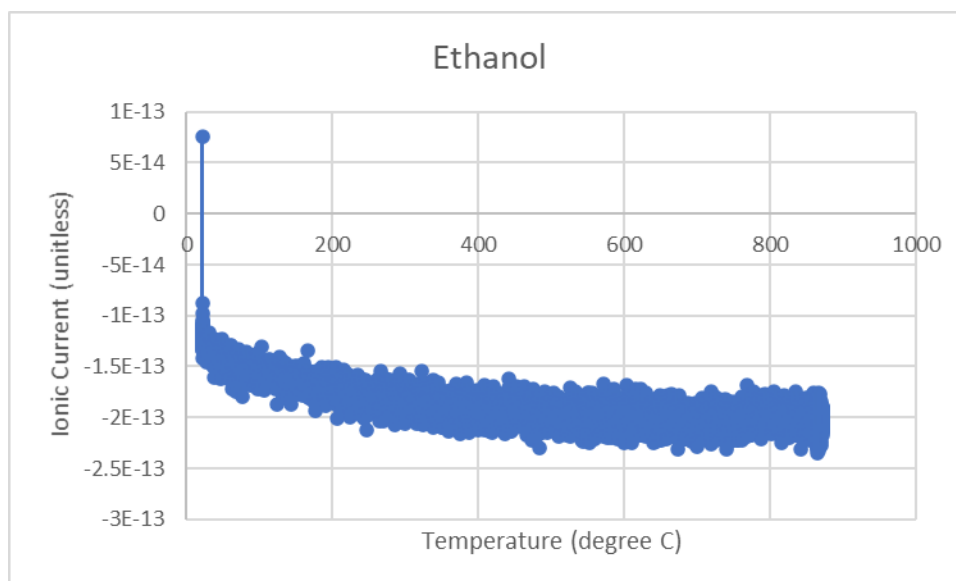
Figure A 40: 2% CO_2 Ethanol TPD (sample 7-20 result)
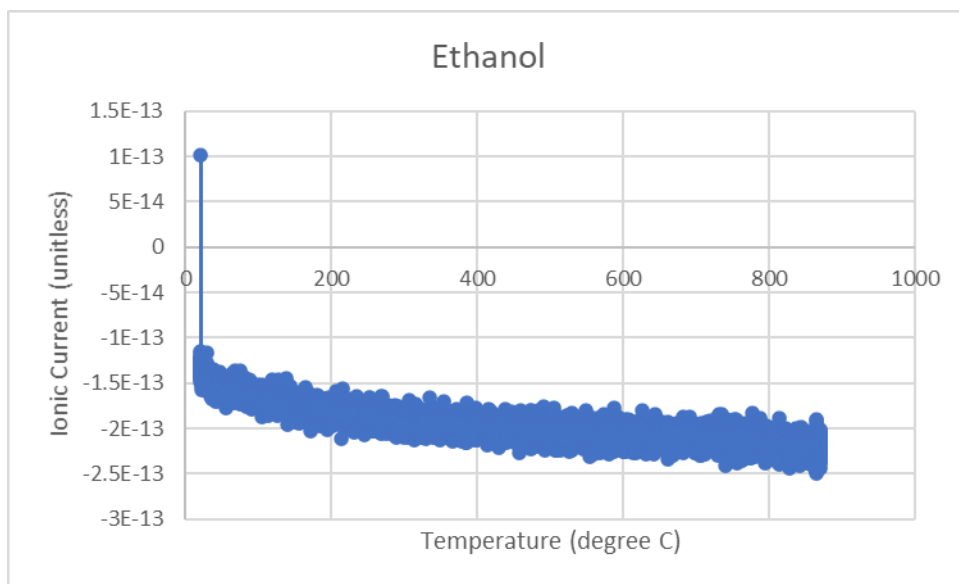
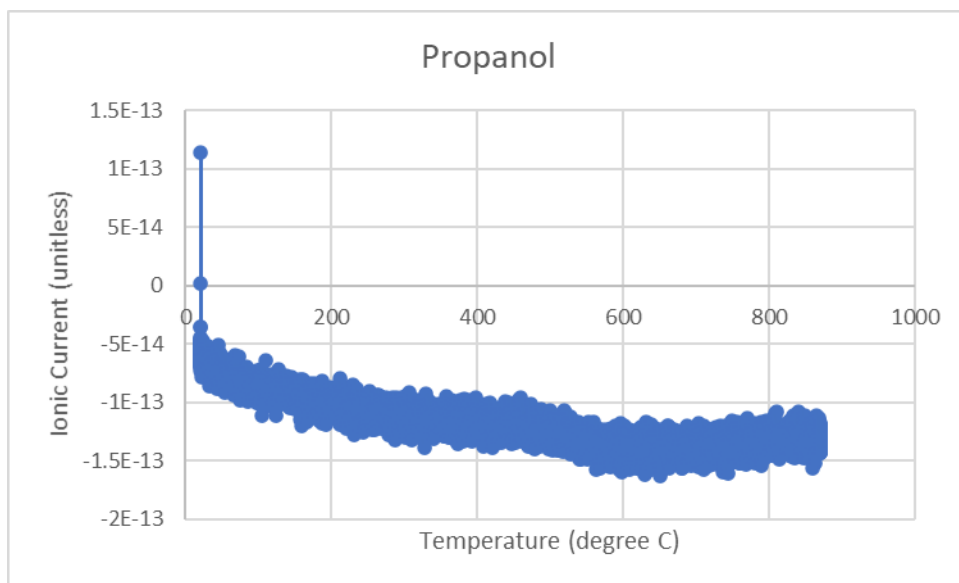*Figure A 41: 3% CO_2 Ethanol TPD (sample 7-22 result)*

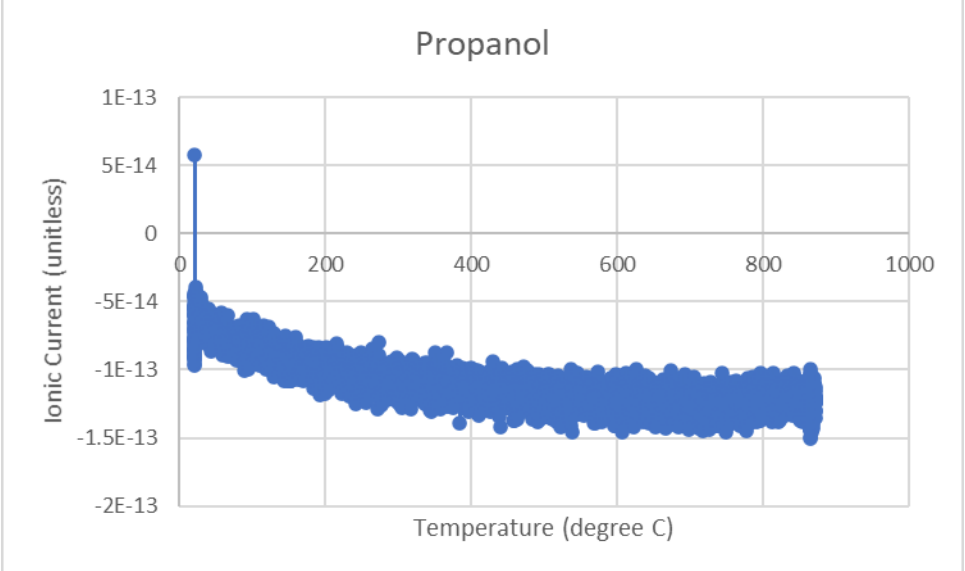*Figure A 42: 1% CO_2 Propanol TPD (sample 7-07 result)*

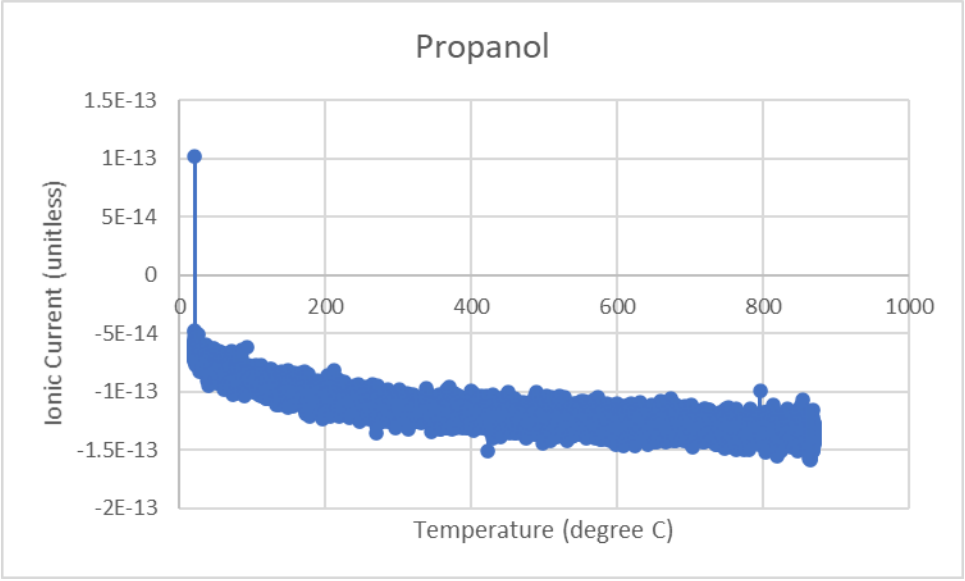Figure A 43: 2% CO_2 Propanol TPD (sample 7-20 result)
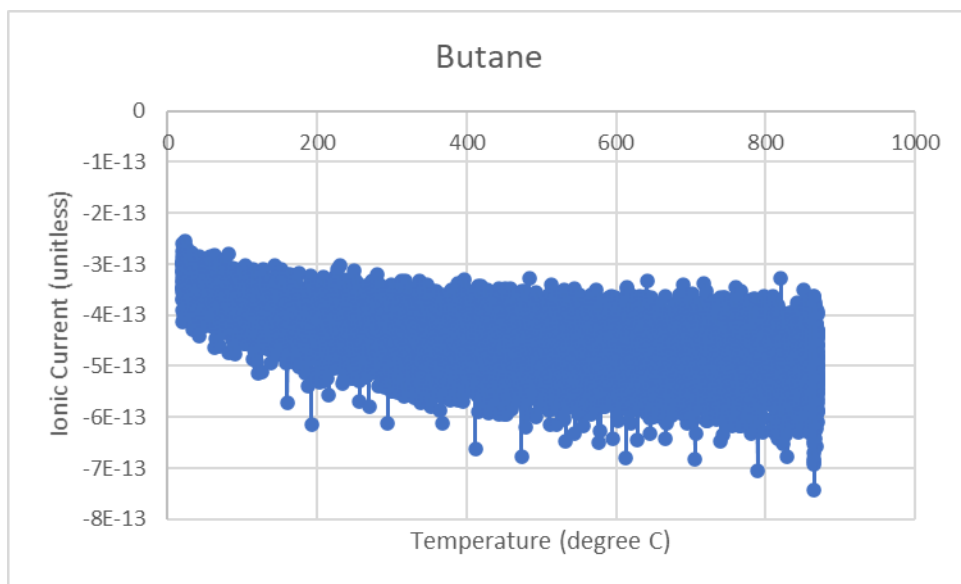

Figure A 44: 3% CO_2 Propanol TPD (sample 7-22 result)
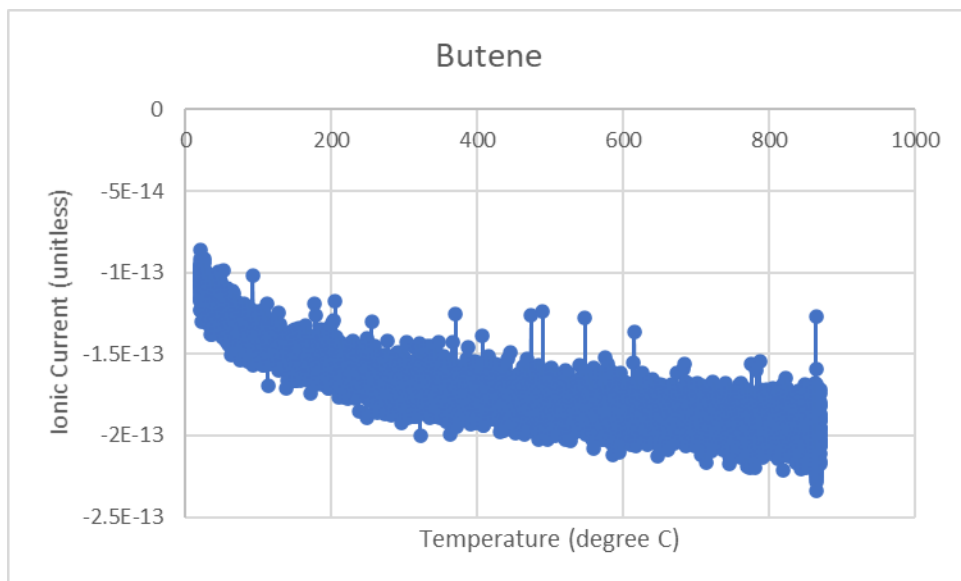
Figure A 45: 3% CO_2 Butane TPD (sample 7-22 result)

Figure A 46: 3% CO_2 Butene TPD (sample 7-22 result)
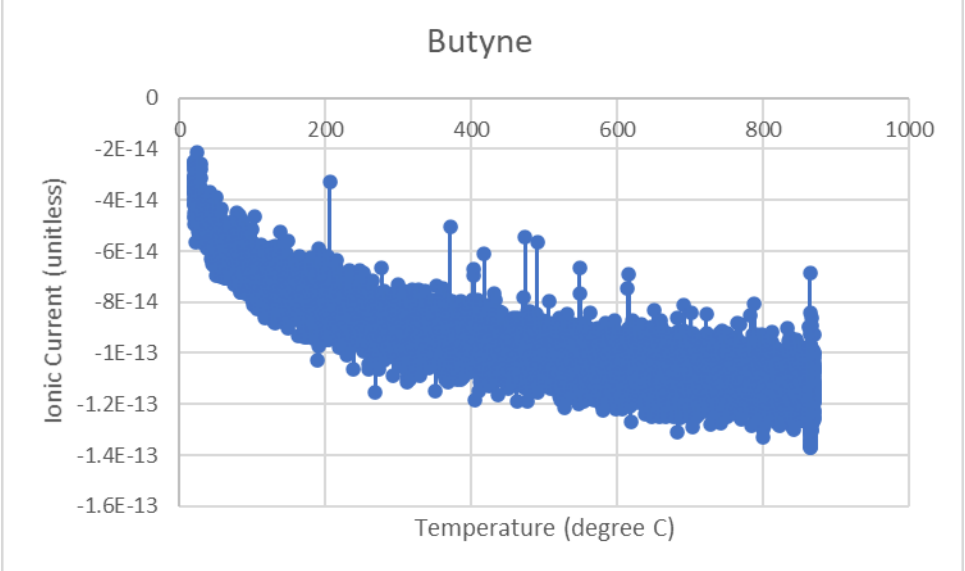
Figure A 47: 3% CO_2 Butyne TPD (sample 7-22 result)

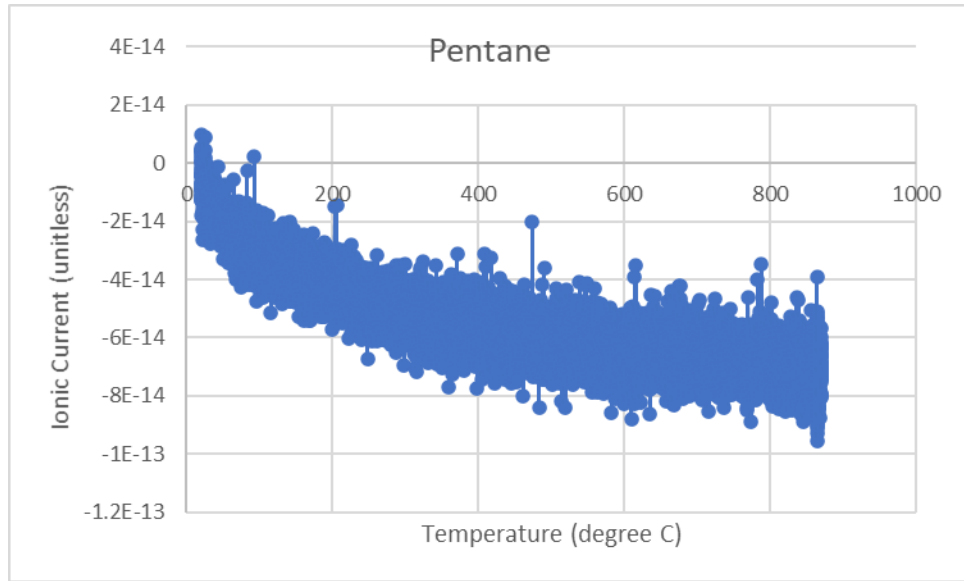*Figure A 48: 3% CO_2 Pentane TPD (sample 7-22 result)*

Figure A 49: 2% CO_2 Propyne TPD (sample 7-20 result)

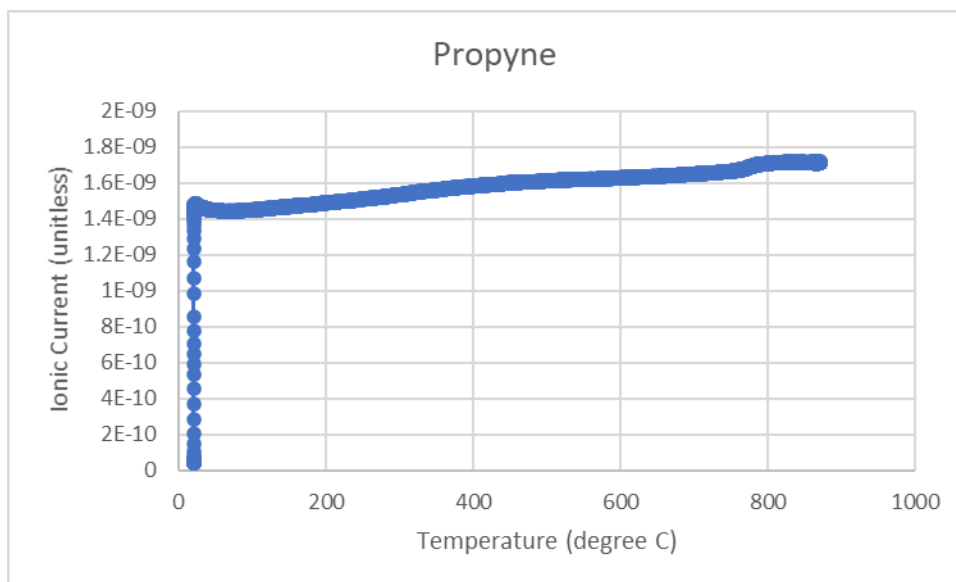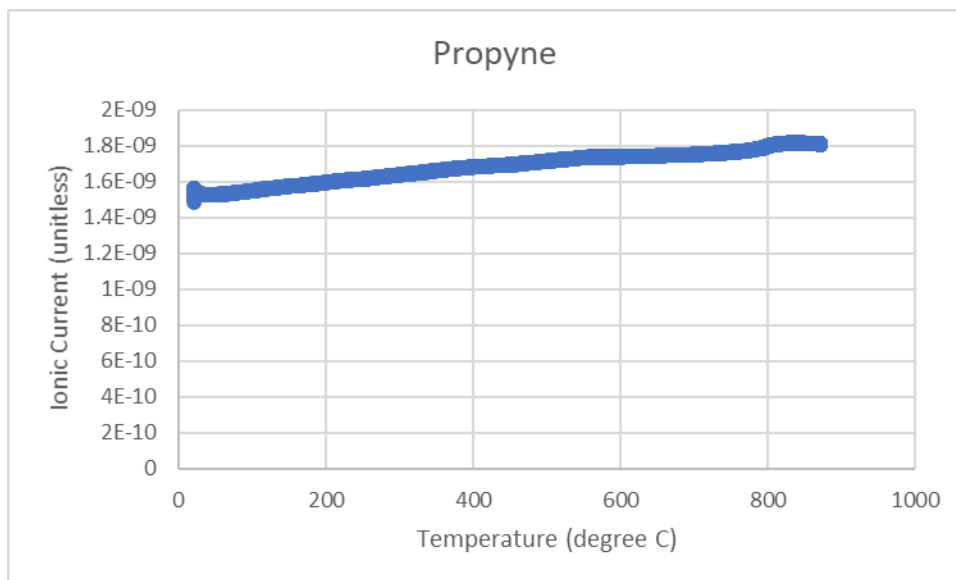*Figure A 50: 1% CO_2 Propyne TPD (sample 7-07 result)*
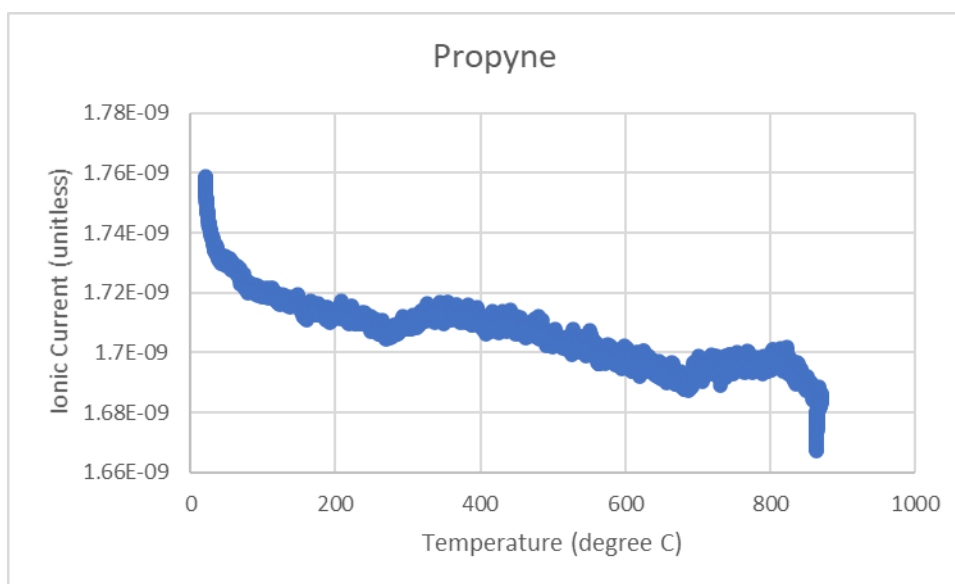
Figure A 51: 3% CO_2 Propyne TPD (sample 7-22 result)
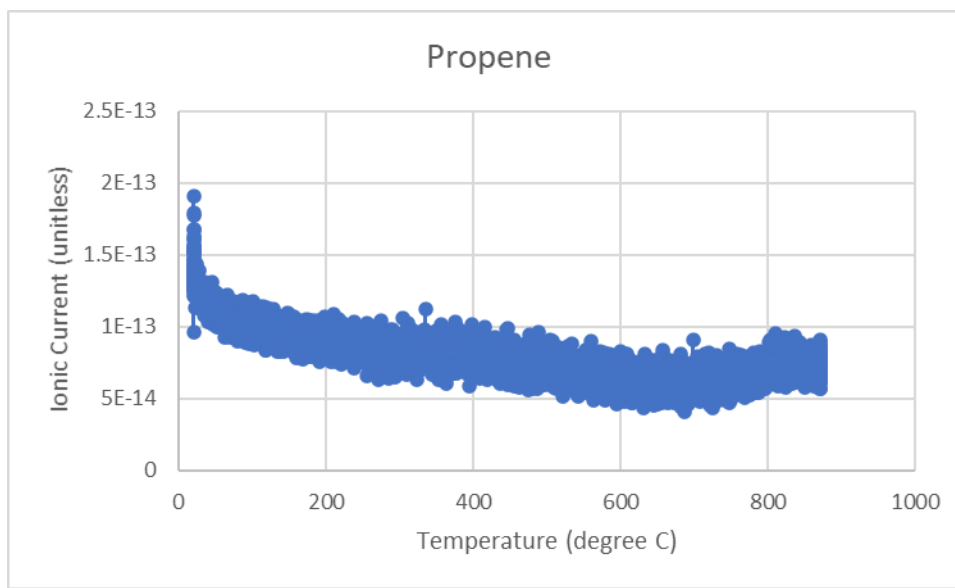
Figure A 52: 1% CO_2 Propene TPD (sample 7-07 result)
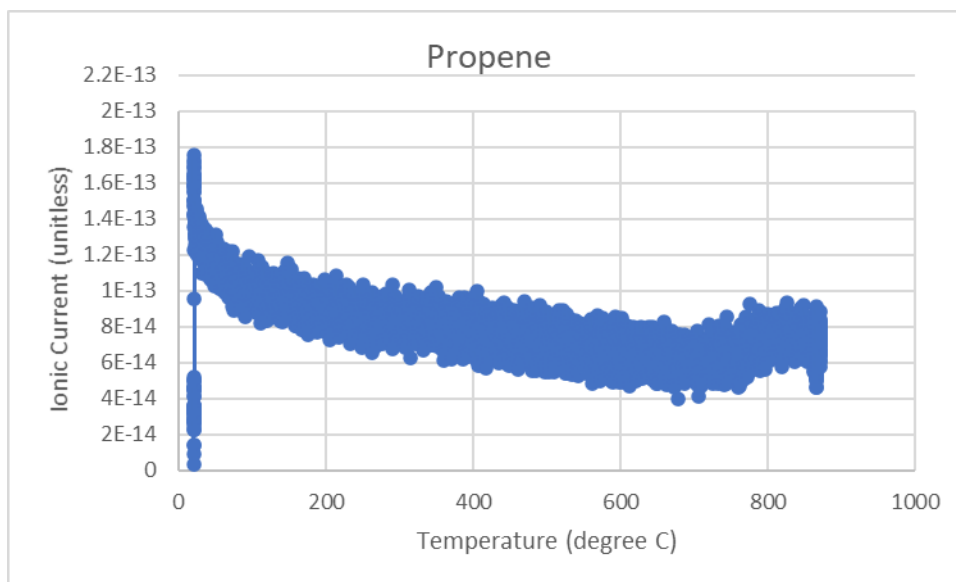
Figure A 53: 2% CO_2 Propene TPD (sample 7-20 result)
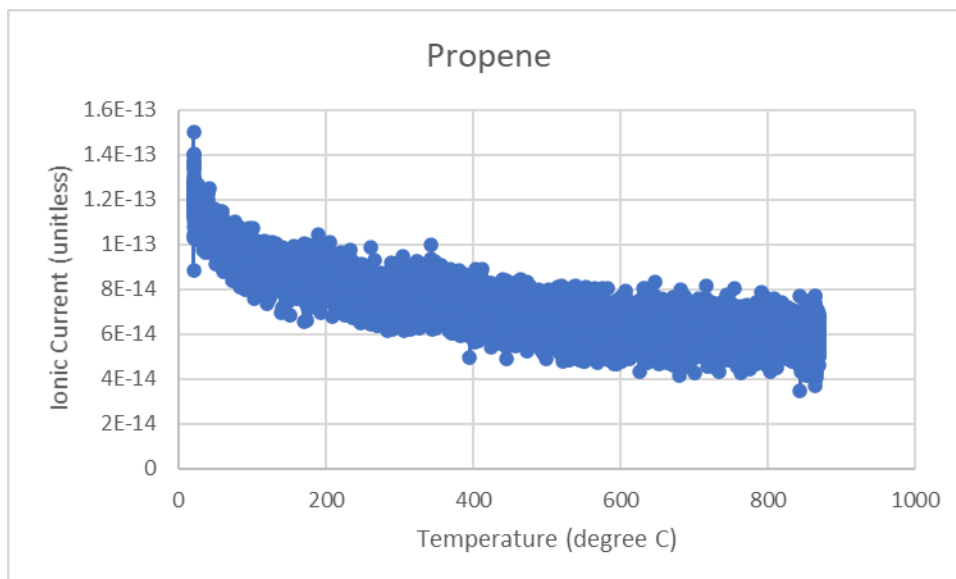
Figure A 54: 3% CO_2 Propene TPD (sample 7-22 result)
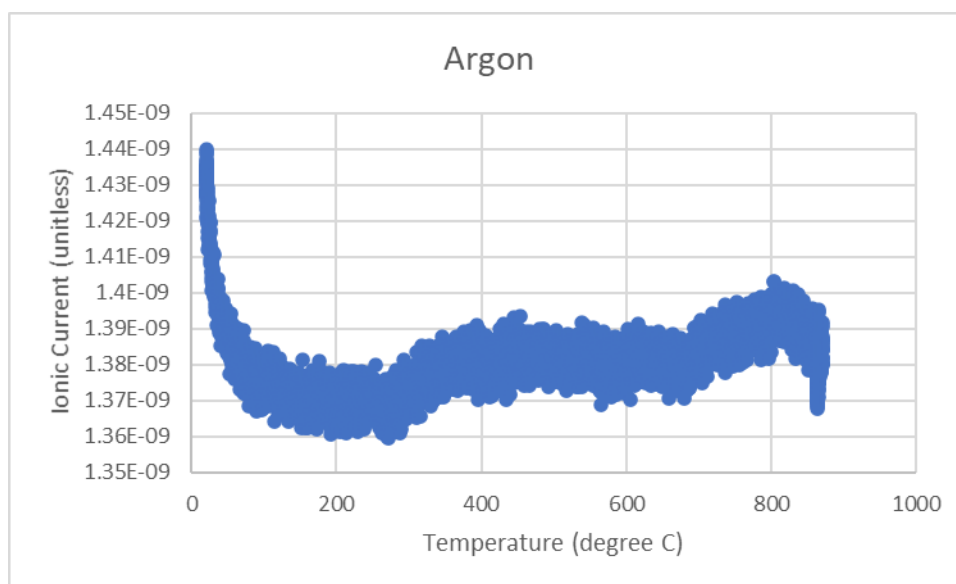
Figure A 55: 3% CO_2 Argon TPD (sample 7-22 result)
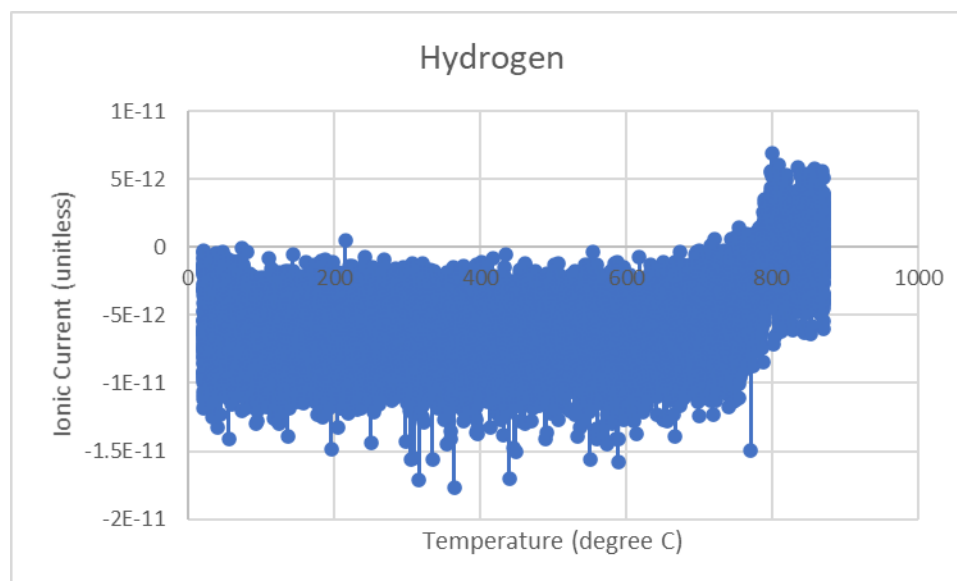
Figure A 56: 1% CO_2 Hydrogen TPD (sample 7-07 result)
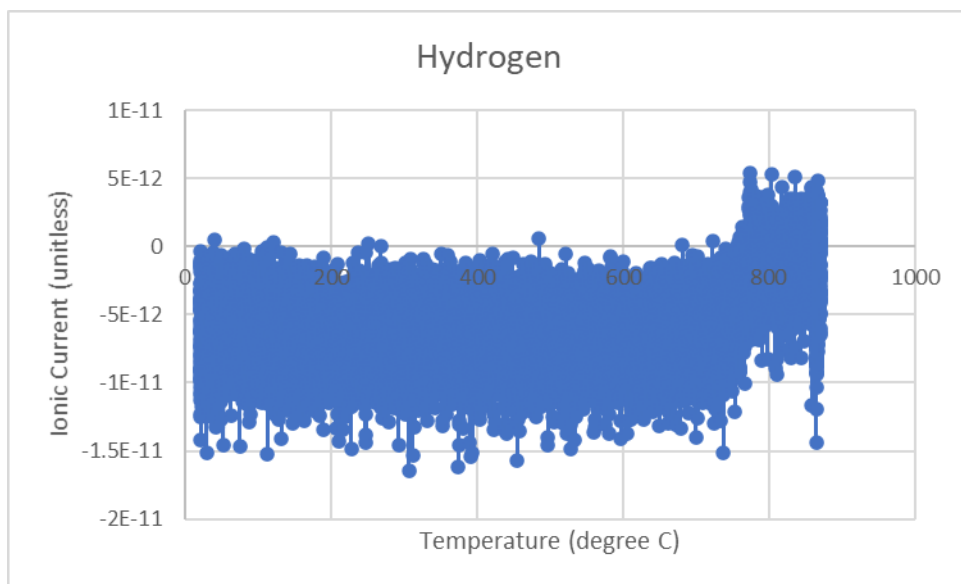
Figure A 57: 2% CO_2 Hydrogen TPD (sample 7-20 result)
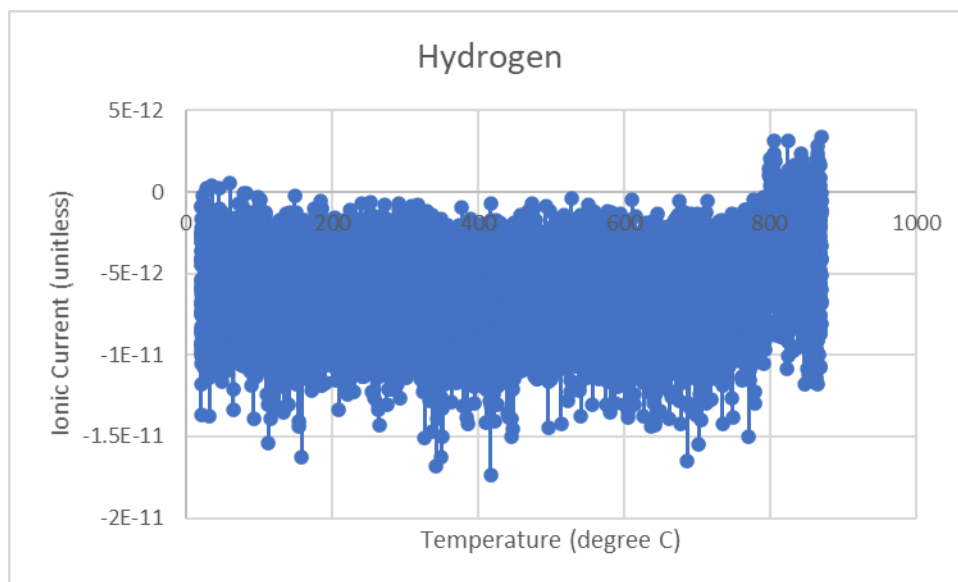
Figure A 58: 3% CO_2 Hydrogen TPD (sample 7-22 result)
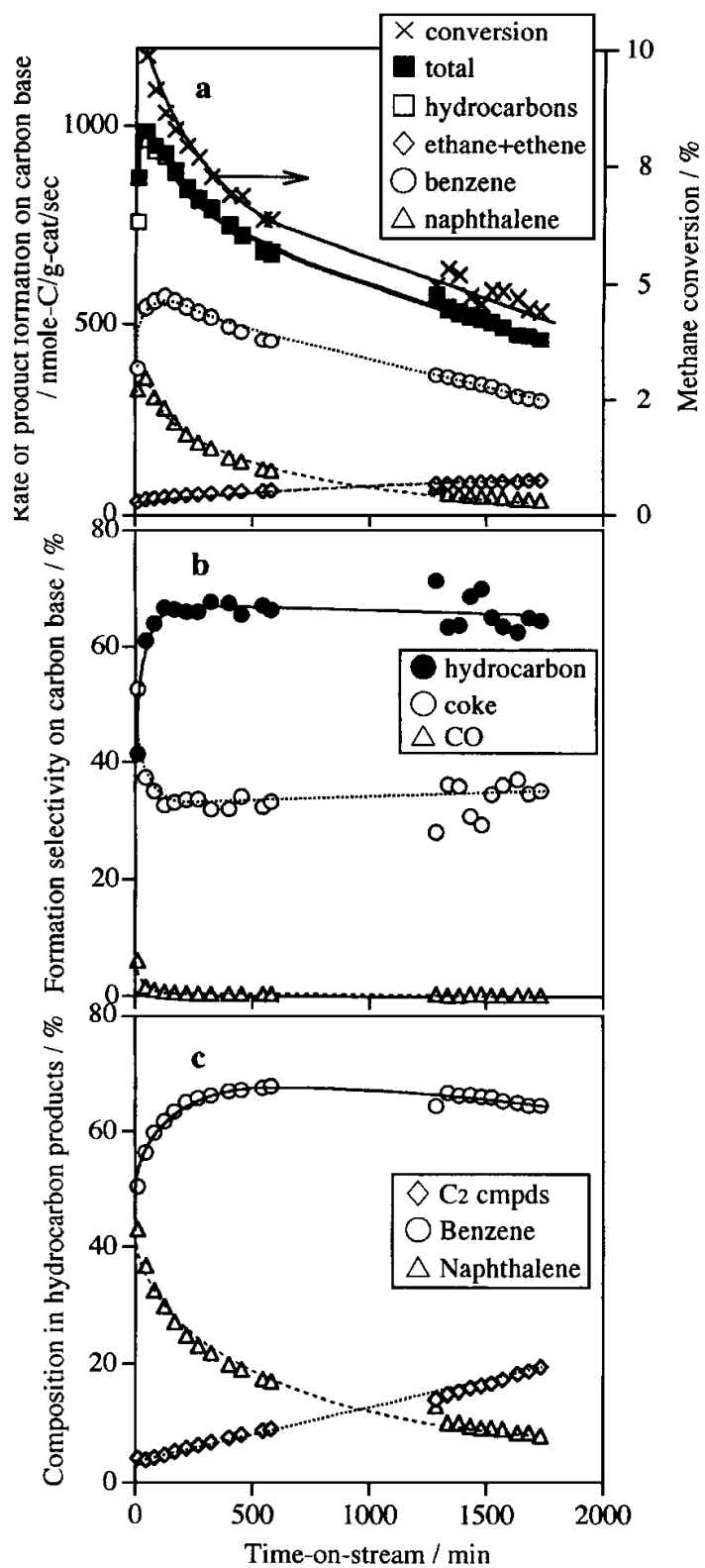
Figure A 59: Ohnishi's Baseline Molybdenum Catalyst Results

methane only(✕), +1.6%CO2(◯), +4.1%CO2(⊕),+12%CO2(●)
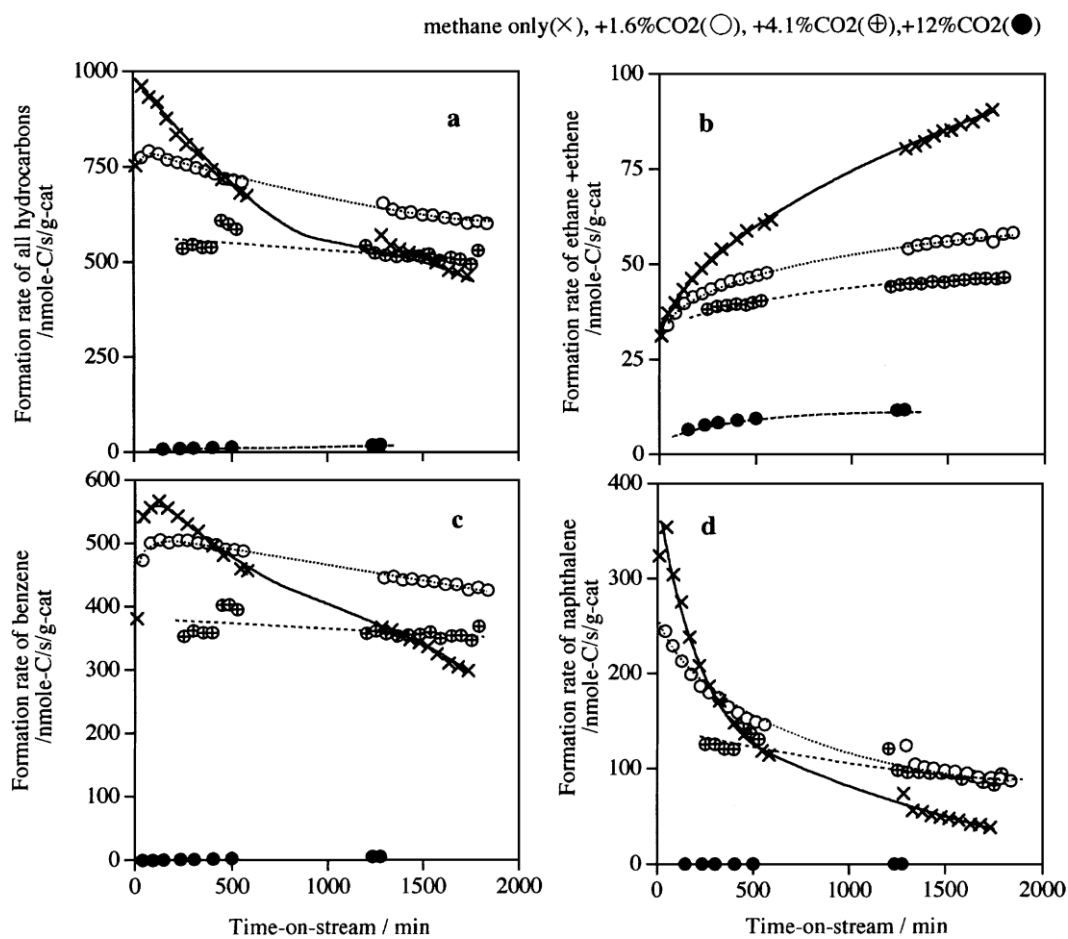
Figure A 60: Ohnishi's Carbon Dioxide Results

Appendix B: Other Experimental Data
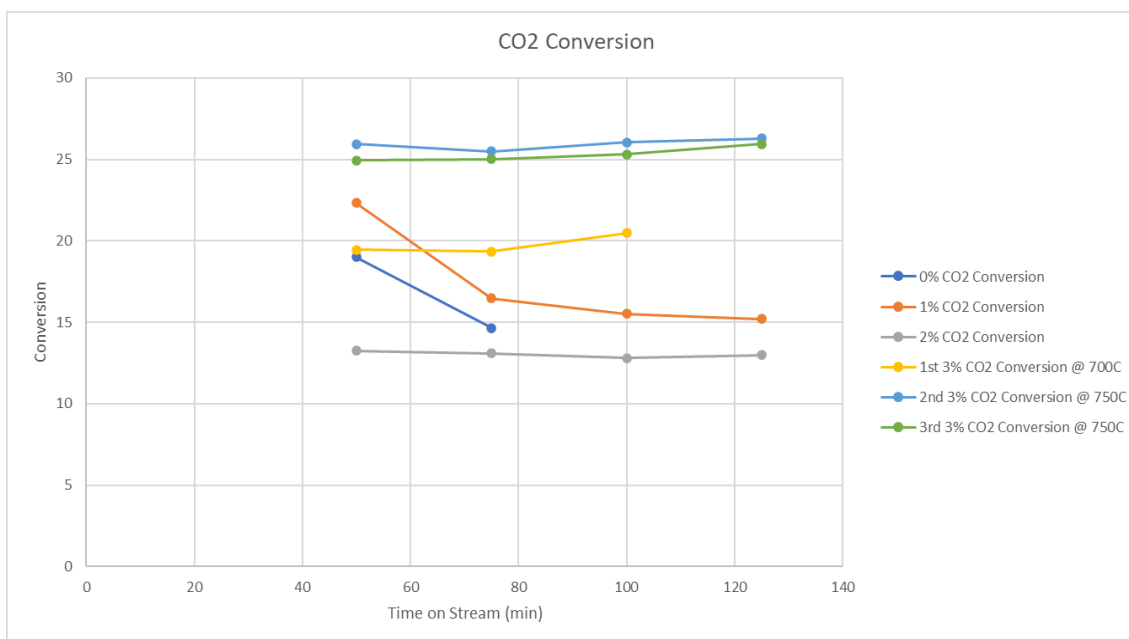
Figure B 61: 2 hour Methane Conversion using 2 wt% Molybdenum Catalyst
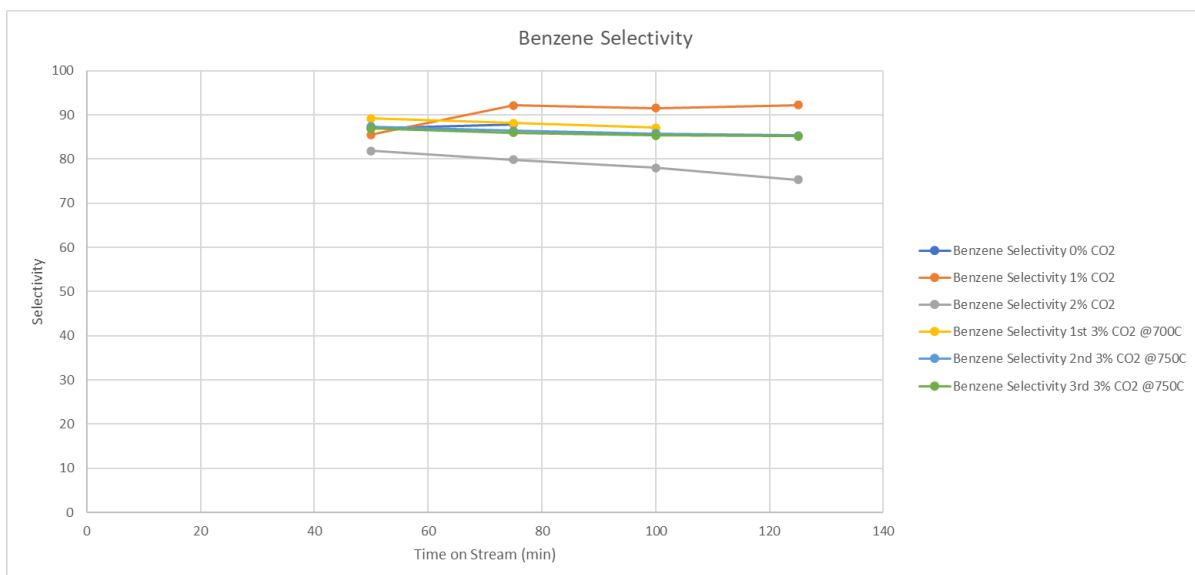
Figure B 62: 2 Hour Benzene Selectivity using 2 wt% Molybdenum Catalyst
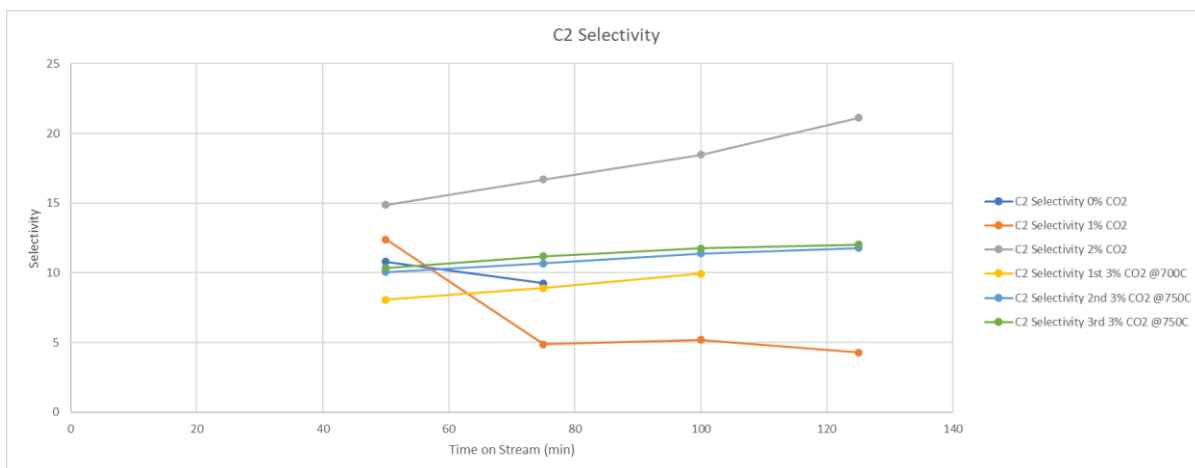
Figure B 63: 2 Hour C_2 Selectivity using 2 wt% Molybdenum Catalyst
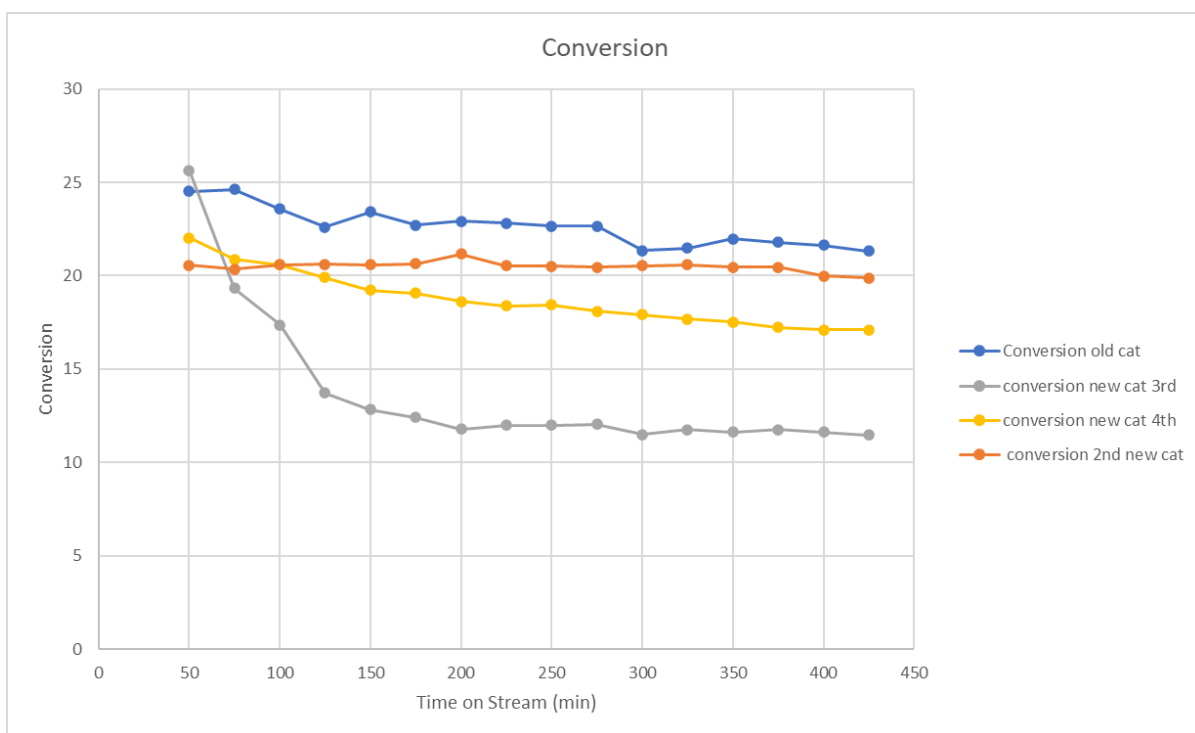
Figure B 64: 6 Hour Methane Conversion with varied 2 wt% Molybdenum Catalysts
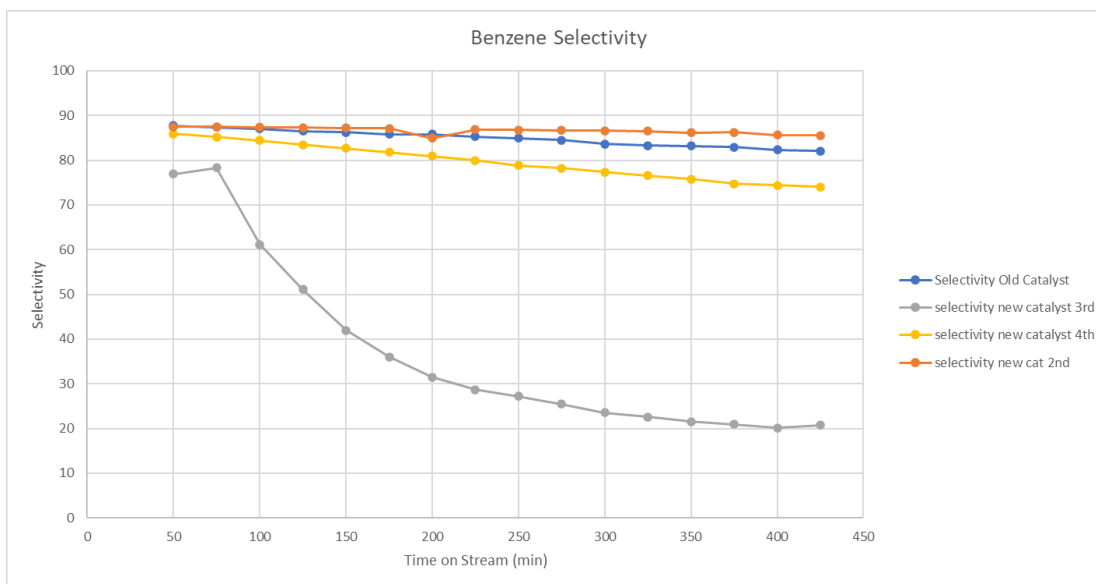
Figure B 65: 6 Hour Benzene Selectivity with varied 2 wt% Molybdenum Catalysts
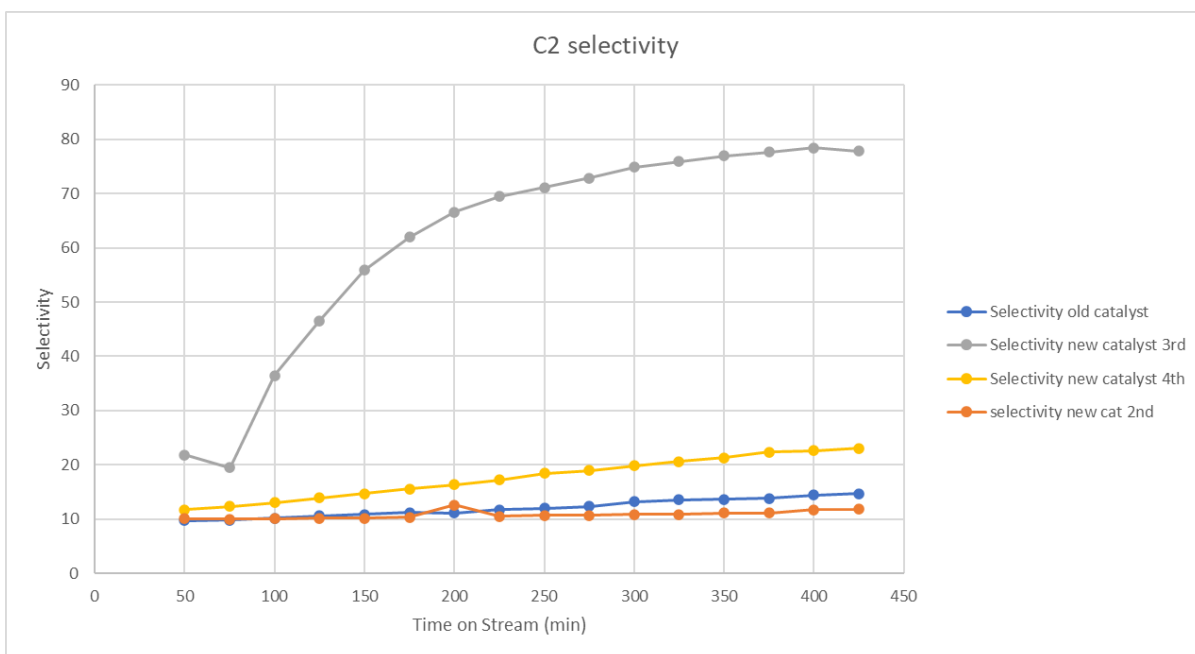
Figure B 66: 6 Hour C_2 Selectivity with varied 2 wt% Molybdenum Catalysts

References

(1) M W Browne. A Pervasive Molecule Is Captured in a Photograph. *The New York Times* **1988**.

(2) Nithyanandam, R.; Mun, Y. K.; Fong, T. S.; Siew, T. C.; Yee, O. S.; Ismail, N. Review on Production of Benzene from Petroleum Associated Gas by Dehydro-Aromatization, Partial Oxidation of Methane and Methanol-to-Aromatics Process. **2018**, *13*, 21.

(3) Ed Dlugokencky. Parts per Billion of Methane within the Air. *NOAA ESRL Global Monitoring Laboratory* **2021**.

(4) Mandy Curnow. Carbon Farming: Reducing Methane Emissions from Cattle Using Feed Additives. *Department of Agriculture* **2021**.

(5) Krulwich, R. A Mysterious Patch of Light Shows up in the North Dakota Dark. *National Public Radio,* **2013**.

(6) Wang, L.; Tao, L.; Xie, M.; Xu, G.; Huang, J.; Xu, Y. Dehydrogenation and Aromatization of Methane under Non-Oxidizing Conditions. *Catal Lett* **1993**, *21* (1–2), 35–41. https://doi.org/10.1007/BF00767368.

(7) Denardin, F. G.; Perez-Lopez, O. W. Methane Dehydroaromatization over Fe-M/ZSM-5 Catalysts (M= Zr, Nb, Mo). *Microporous and Mesoporous Materials* **2020**, *295*, 109961. https://doi.org/10.1016/j.micromeso.2019.109961.

(8) Gu, Y.; Chen, P.; Wang, X.; Lyu, Y.; Liu, W.; Liu, X.; Yan, Z. Active Sites and Induction Period of Fe/ZSM-5 Catalyst in Methane Dehydroaromatization. *ACS Catal.* **2021**, *11* (12), 6771–6786. https://doi.org/10.1021/acscatal.1c01467.

(9) Denardin, F.; Perez-Lopez, O. W. Tuning the Acidity and Reducibility of Fe/ZSM-5 Catalysts for Methane Dehydroaromatization. *Fuel* **2019**, *236*, 1293–1300. https://doi.org/10.1016/j.fuel.2018.09.128.

(10) Wang, K.; Huang, X.; Li, D. Hollow ZSM-5 Zeolite Grass Ball Catalyst in Methane Dehydroaromatization: One-Step Synthesis and the Exceptional Catalytic Performance. *Applied Catalysis A: General* **2018**, *556*, 10–19. https://doi.org/10.1016/j.apcata.2018.02.030.

(11) Ohnishi, R.; Liu, S.; Dong, Q.; Wang, L.; Ichikawa, M. Catalytic Dehydrocondensation of Methane with CO and CO_2 toward Benzene and Naphthalene on Mo/HZSM-5 and Fe/Co-Modified Mo/HZSM-5. *Journal of Catalysis* **1999**, *182* (1), 92–103. https://doi.org/10.1006/jcat.1998.2319.

(12) Kosinov, N.; Coumans, F. J. A. G.; Uslamin, E. A.; Wijpkema, A. S. G.; Mezari, B.; Hensen, E. J. M. Methane Dehydroaromatization by Mo/HZSM-5: Mono- or Bifunctional Catalysis? *ACS Catal.* **2017**, *7* (1), 520–529. https://doi.org/10.1021/acscatal.6b02497.

(13) Matus, E. V.; Ismagilov, I. Z.; Sukhova, O. B.; Zaikovskii, V. I.; Tsikoza, L. T.; Ismagilov, Z. R.; Moulijn, J. A. Study of Methane Dehydroaromatization on Impregnated Mo/ZSM-5 Catalysts and Characterization of Nanostructured Molybdenum Phases and Carbonaceous Deposits. *Ind. Eng. Chem. Res.* **2007**, *46* (12), 4063–4074. https://doi.org/10.1021/ie0609564.

(14) Ramirez-Mendoza, H.; Valdez Lancinha Pereira, M.; Van Gerven, T.; Lutz, C.; Julian, I. Ultrasound-Assisted Preparation of Mo/ZSM-5 Zeolite Catalyst for Non-Oxidative Methane Dehydroaromatization. *Catalysts* **2021**, *11* (3), 313. https://doi.org/10.3390/catal11030313.

(15) Tian, M.; Zhao, T. Q.; Chin, P. L.; Liu, B. S.; Cheung, A. S.-C. Methane and Propane Co-Conversion Study over Zinc, Molybdenum and Gallium Modified HZSM-5 Catalysts Using Time-of-Flight Mass-Spectrometry. *Chemical Physics Letters* **2014**, *592*, 36–40. https://doi.org/10.1016/j.cplett.2013.12.001.

(16) Bedard, J.; Hong, D.-Y.; Bhan, A. CH_4 Dehydroaromatization on Mo/H–ZSM-5: 1. Effects of Co-Processing H_2 and CH_3COOH. *Journal of Catalysis* **2013**, *306*, 58–67. https://doi.org/10.1016/j.jcat.2013.06.003.

(17) Balyan, S.; Haider, M. A.; Khan, T. S.; Pant, K. K. Boric Acid Treated HZSM-5 for Improved Catalyst Activity in Non-Oxidative Methane Dehydroaromatization. *Catal. Sci. Technol.* **2020**, *10* (12), 3857–3867. https://doi.org/10.1039/D0CY00286K.

(18) Julian, I.; Hueso, J. L.; Lara, N.; Solé-Daurá, A.; Poblet, J. M.; Mitchell, S. G.; Mallada, R.; Santamaría, J. Polyoxometalates as Alternative Mo Precursors for Methane Dehydroaromatization on Mo/ZSM-5 and Mo/MCM-22 Catalysts. *Catal. Sci. Technol.* **2019**, *9* (21), 5927–5942. https://doi.org/10.1039/C9CY01490J.

(19) Mamonov, N. A.; Fadeeva, E. V.; Grigoriev, D. A.; Mikhailov, M. N.; Kustov, L. M.; Alkhimov, S. A. Metal/Zeolite Catalysts of Methane Dehydroaromatization. *Russ. Chem. Rev.* **2013**, *82* (6), 567–585. https://doi.org/10.1070/RC2013v082n06ABEH004346.

(20) Vollmer, I.; Li, G.; Yarulina, I.; Kosinov, N.; Hensen, E. J.; Houben, K.; Mance, D.; Baldus, M.; Gascon, J.; Kapteijn, F. Relevance of the Mo-Precursor State in H-ZSM-5 for Methane Dehydroaromatization. *Catal. Sci. Technol.* **2018**, *8* (3), 916–922. https://doi.org/10.1039/C7CY01789H.

(21) Colket, M. B.; Seery, D. J. Reaction Mechanisms for Toluene Pyrolysis. *Symposium (International) on Combustion* **1994**, *25* (1), 883–891. https://doi.org/10.1016/S0082-0784(06)80723-X.

(22) Schwartz, D.; Gadiou, R.; Brilhac, J.-F.; Prado, G.; Martinez, G. A Kinetic Study of the Decomposition of Spent Sulfuric Acids at High Temperature. *Ind. Eng. Chem. Res.* **2000**, *39* (7), 2183–2189. https://doi.org/10.1021/ie990801e.

(23) Yokoi, T.; Tsusaka, A.; Matsumura, T.; Yukita, K.; Goto, Y.; Yokomizu, Y. Dependence of Critical Electric Field Strength in High Temperature CO_2 Gas on Contamination of PTFE Vapor. In *2019 5th International Conference on Electric Power Equipment - Switching Technology (ICEPE-ST)*; IEEE: Kitakyushu, Japan, 2019; pp 97–100. https://doi.org/10.1109/ICEPE-ST.2019.8928934.

(24) Klein, D. R. *Organic Chemistry*, Second edition.; Wiley: Hoboken, NJ, 2015.

(25) Fogler, H. S. *Elements of Chemical Reaction Engineering*, Fifth edition.; Prentice Hall: Boston, 2016.

(26) Huang, K.; Miller, J. B.; Huber, G. W.; Dumesic, J. A.; Maravelias, C. T. A General Framework for the Evaluation of Direct Nonoxidative Methane Conversion Strategies. *Joule* **2018**, *2* (2), 349–365. https://doi.org/10.1016/j.joule.2018.01.001.

(27) Kosinov, N.; Hensen, E. J. M. Zeolite-Based Catalysts: Reactivity, Selectivity, and Stability of Zeolite-Based Catalysts for Methane Dehydroaromatization (Adv. Mater. 44/2020). *Adv. Mater.* **2020**, *32* (44), 2070332. https://doi.org/10.1002/adma.202070332.

(28) Louis, B.; Walspurger, S.; Sommer, J. Quantitative Determination of Brönsted Acid Sites on Zeolites: A New Approach Towards the Chemical Composition of Zeolites.

Catalysis Letters **2004**, *93* (1/2), 81–84.
https://doi.org/10.1023/B:CATL.0000016953.36257.88.

(29) Sim, J. P.; Lee, B. J.; Han, G.-H.; Kim, D. H.; Lee, K.-Y. Promotional Effect of Au on
Fe/HZSM-5 Catalyst for Methane Dehydroaromatization. *Fuel* **2020**, *274*, 117852.
https://doi.org/10.1016/j.fuel.2020.117852.

(30) Rahman, M.; Infantes-Molina, A.; Hoffman, A. S.; Bare, S. R.; Emerson, K. L.; Khatib,
S. J. Effect of Si/Al Ratio of ZSM-5 Support on Structure and Activity of Mo Species in
Methane Dehydroaromatization. *Fuel* **2020**, *278*, 118290.
https://doi.org/10.1016/j.fuel.2020.118290.

(31) Gu, Y.; Chen, P.; Yan, H.; Wang, X.; Lyu, Y.; Tian, Y.; Liu, W.; Yan, Z.; Liu, X.
Coking Mechanism of Mo/ZSM-5 Catalyst in Methane Dehydroaromatization. *Applied
Catalysis A: General* **2021**, *613*, 118019. https://doi.org/10.1016/j.apcata.2021.118019.

(32) Goodarzi, F.; Hansen, L. P.; Helveg, S.; Mielby, J.; Nguyen, T. T. M.; Joensen, F.;
Kegnæs, S. The Catalytic Effects of Sulfur in Ethane Dehydroaromatization. *Chem.
Commun.* **2020**, *56* (40), 5378–5381. https://doi.org/10.1039/D0CC00408A.

(33) Kanitkar, S.; Abedin, M. A.; Bhattar, S.; Spivey, J. J. Methane Dehydroaromatization
over Molybdenum Supported on Sulfated Zirconia Catalysts. *Applied Catalysis A:
General* **2019**, *575*, 25–37. https://doi.org/10.1016/j.apcata.2019.01.013.

(34) Julian, I.; Roedern, M. B.; Hueso, J. L.; Irusta, S.; Baden, A. K.; Mallada, R.; Davis, Z.;
Santamaria, J. Supercritical Solvothermal Synthesis under Reducing Conditions to
Increase Stability and Durability of Mo/ZSM-5 Catalysts in Methane
Dehydroaromatization. *Applied Catalysis B: Environmental* **2020**, *263*, 118360.
https://doi.org/10.1016/j.apcatb.2019.118360.

(35) Zhai, D.; Liu, Y.; Zheng, H.; Zhao, L.; Gao, J.; Xu, C.; Shen, B. A First-Principles
Evaluation of the Stability, Accessibility, and Strength of Brønsted Acid Sites in
Zeolites. *Journal of Catalysis* **2017**, *352*, 627–637.
https://doi.org/10.1016/j.jcat.2017.06.035.

(36) Tshabalala, T. E.; Coville, N. J.; Anderson, J. A.; Scurrell, M. S. Dehydroaromatization
of Methane over Sn–Pt Modified Mo/H-ZSM-5 Zeolite Catalysts: Effect of Preparation
Method. *Applied Catalysis A: General* **2015**, *503*, 218–226.
https://doi.org/10.1016/j.apcata.2015.06.035.

(37) Tshabalala, T. E.; Coville, N. J.; Scurrell, M. S. Methane Dehydroaromatization over
Modified Mn/H-ZSM-5 Zeolite Catalysts: Effect of Tungsten as a Secondary Metal.
Catalysis Communications **2016**, *78*, 37–43.
https://doi.org/10.1016/j.catcom.2016.02.005.

(38) Thakur, R.; Hoffman, M.; VahidMohammadi, A.; Smith, J.; Chi, M.; Tatarchuk, B.;
Beidaghi, M.; Carrero, C. A. Multilayered Two-Dimensional $V_2 CT_x$ MXene for
Methane Dehydroaromatization. *ChemCatChem* **2020**, *12* (14), 3639–3643.
https://doi.org/10.1002/cctc.201902366.

(39) López-Martín, A.; Caballero, A.; Colón, G. Structural and Surface Considerations on
Mo/ZSM-5 Systems for Methane Dehydroaromatization Reaction. *Molecular Catalysis*
2020, *486*, 110787. https://doi.org/10.1016/j.mcat.2020.110787.

(40) Zhu, P.; Yang, G.; Sun, J.; Fan, R.; Zhang, P.; Yoneyama, Y.; Tsubaki, N. A Hollow
Mo/HZSM-5 Zeolite Capsule Catalyst: Preparation and Enhanced Catalytic Properties

in Methane Dehydroaromatization. *J. Mater. Chem. A* **2017**, *5* (18), 8599–8607. https://doi.org/10.1039/C7TA02345F.

(41) Abdelsayed, V.; Smith, M. W.; Shekhawat, D. Investigation of the Stability of Zn-Based HZSM-5 Catalysts for Methane Dehydroaromatization. *Applied Catalysis A: General* **2015**, *505*, 365–374. https://doi.org/10.1016/j.apcata.2015.08.017.

(42) Denardin, F. G.; Muniz, A. R.; Perez-Lopez, O. W. Nature of the Interactions between Fe and Zr for the Methane Dehydroaromatization Reaction in ZSM-5. *Journal of Molecular Structure* **2020**, *1220*, 128720. https://doi.org/10.1016/j.molstruc.2020.128720.

(43) Xu, B.; Sievers, C.; Hong, S.; Prins, R.; Vanbokhoven, J. Catalytic Activity of Brønsted Acid Sites in Zeolites: Intrinsic Activity, Rate-Limiting Step, and Influence of the Local Structure of the Acid Sites. *Journal of Catalysis* **2006**, *244* (2), 163–168. https://doi.org/10.1016/j.jcat.2006.08.022.

(44) Karakaya, C.; Zhu, H.; Kee, R. J. Kinetic Modeling of Methane Dehydroaromatization Chemistry on Mo/Zeolite Catalysts in Packed-Bed Reactors. *Chemical Engineering Science* **2015**, *123*, 474–486. https://doi.org/10.1016/j.ces.2014.11.039.

(45) Li, G.; Vollmer, I.; Liu, C.; Gascon, J.; Pidko, E. A. Structure and Reactivity of the Mo/ZSM-5 Dehydroaromatization Catalyst: An Operando Computational Study. *ACS Catal.* **2019**, *9* (9), 8731–8737. https://doi.org/10.1021/acscatal.9b02213.

(46) Rahman, M.; Infantes-Molina, A.; Boubnov, A.; Bare, S. R.; Stavitski, E.; Sridhar, A.; Khatib, S. J. Increasing the Catalytic Stability by Optimizing the Formation of Zeolite-Supported Mo Carbide Species Ex Situ for Methane Dehydroaromatization. *Journal of Catalysis* **2019**, *375*, 314–328. https://doi.org/10.1016/j.jcat.2019.06.002.

(47) Matus, E. V.; Ismagilov, I. Z.; Sukhova, O. B.; Zaikovskii, V. I.; Tsikoza, L. T.; Ismagilov, Z. R.; Moulijn, J. A. Study of Methane Dehydroaromatization on Impregnated Mo/ZSM-5 Catalysts and Characterization of Nanostructured Molybdenum Phases and Carbonaceous Deposits. *Ind. Eng. Chem. Res.* **2007**, *46* (12), 4063–4074. https://doi.org/10.1021/ie0609564.

(48) Abedin, M. A.; Kanitkar, S.; Bhattar, S.; Spivey, J. J. Promotional Effect of Cr in Sulfated Zirconia-Based Mo Catalyst for Methane Dehydroaromatization. *Energy Technol.* **2020**, *8* (8), 1900555. https://doi.org/10.1002/ente.201900555.

(49) Bao, H.; Chen, X.; Fang, J.; Jiang, Z.; Huang, W. Structure-Activity Relation of Fe2O3–CeO2 Composite Catalysts in CO Oxidation. *Catal Lett* **2008**, *125* (1–2), 160–167. https://doi.org/10.1007/s10562-008-9540-3.

(50) Liu, B.; Yang, Y.; Sayari, A. Non-Oxidative Dehydroaromatization of Methane over Ga-Promoted Mo/HZSM-5-Based Catalysts. *Applied Catalysis A: General* **2001**, *214* (1), 95–102. https://doi.org/10.1016/S0926-860X(01)00470-7.

(51) Li, L.; Mu, X.; Liu, W.; Kong, X.; Fan, S.; Mi, Z.; Li, C.-J. Thermal Non-Oxidative Aromatization of Light Alkanes Catalyzed by Gallium Nitride. *Angew. Chem.* **2014**, *126* (51), 14330–14333. https://doi.org/10.1002/ange.201408754.

(52) Abedin, M. A.; Kanitkar, S.; Bhattar, S.; Spivey, J. J. Sulfated Hafnia as a Support for Mo Oxide: A Novel Catalyst for Methane Dehydroaromatization. *Catalysis Today* **2020**, *343*, 8–17. https://doi.org/10.1016/j.cattod.2019.02.021.

(53) Cheng, X.; Yan, P.; Zhang, X.; Yang, F.; Dai, C.; Li, D.; Ma, X.-X. Enhanced Methane Dehydroaromatization in the Presence of CO_2 over Fe- and Mg-Modified Mo/ZSM-5. *Molecular Catalysis* **2017**, *437*, 114–120. https://doi.org/10.1016/j.mcat.2017.05.011.

(54) Lim, T. H.; Kim, D. H. Characteristics of Mn/H-ZSM-5 Catalysts for Methane Dehydroaromatization. *Applied Catalysis A: General* **2019**, *577*, 10–19. https://doi.org/10.1016/j.apcata.2019.03.008.

(55) Kosinov, N.; Wijpkema, A. S. G.; Uslamin, E.; Rohling, R.; Coumans, F. J. A. G.; Mezari, B.; Parastaev, A.; Poryvaev, A. S.; Fedin, M. V.; Pidko, E. A.; Hensen, E. J. M. Confined Carbon Mediating Dehydroaromatization of Methane over Mo/ZSM-5. *Angew. Chem. Int. Ed.* **2018**, *57* (4), 1016–1020. https://doi.org/10.1002/anie.201711098.

(56) Song, C.; Gim, M. Y.; Lim, Y. H.; Kim, D. H. Enhanced Yield of Benzene, Toulene, and Xylene from the Co-Aromatization of Methane and Propane over Gallium Supported on Mesoporous ZSM-5 and ZSM-11. *Fuel* **2019**, *251*, 404–412. https://doi.org/10.1016/j.fuel.2019.04.079.

(57) Kang, M. Catalytic Carbon Monoxide Oxidation over CoO_x/CeO_2 Composite Catalysts. *Applied Catalysis A: General* **2003**, *251* (1), 143–156. https://doi.org/10.1016/S0926-860X(03)00324-7.

(58) Liu, R.; Li, F.; Chen, C.; Song, Q.; Zhao, N.; Xiao, F. Nitrogen-Functionalized Reduced Graphene Oxide as Carbocatalysts with Enhanced Activity for Polyaromatic Hydrocarbon Hydrogenation. *Catal. Sci. Technol.* **2017**, *7* (5), 1217–1226. https://doi.org/10.1039/C7CY00058H.

(59) Böhm, H.; Jander, H. PAH Formation in Acetylene–Benzene Pyrolysis. *Phys. Chem. Chem. Phys.* **1999**, *1* (16), 3775–3781. https://doi.org/10.1039/a903306h.

(60) Tani, M.; Sakamoto, T.; Mita, S.; Sakaguchi, S.; Ishii, Y. Hydroxylation of Benzene to Phenol under Air and Carbon Monoxide Catalyzed by Molybdovanadophosphoric Acid. *Angew. Chem. Int. Ed.* **2005**, *44* (17), 2586–2588. https://doi.org/10.1002/anie.200462769.

(61) Nishina, Y.; Takami, K. Bromination of Aromatic Compounds Using an Fe_2O_3/Zeolite Catalyst. *Green Chem.* **2012**, *14* (9), 2380. https://doi.org/10.1039/c2gc35821b.

(62) Vollmer, I.; van der Linden, B.; Ould-Chikh, S.; Aguilar-Tapia, A.; Yarulina, I.; Abou-Hamad, E.; Sneider, Y. G.; Olivos Suarez, A. I.; Hazemann, J.-L.; Kapteijn, F.; Gascon, J. On the Dynamic Nature of Mo Sites for Methane Dehydroaromatization. *Chem. Sci.* **2018**, *9* (21), 4801–4807. https://doi.org/10.1039/C8SC01263F.

(63) Guisnet, M.; Magnoux, P. Organic Chemistry of Coke Formation. *Applied Catalysis A: General* **2001**, *212* (1–2), 83–96. https://doi.org/10.1016/S0926-860X(00)00845-0.

(64) Ma, H.; Ohnishi, R.; Ichikawa, M. Highly Stable Performance of Methane Dehydroaromatization on Mo/HZSM-5 Catalyst with a Small Amount of H_2 Addition into Methane Feed. 4.

(65) Mevawala, C.; Bai, X.; Kotamreddy, G.; Bhattacharyya, D.; Hu, J. Multiscale Modeling of a Direct Nonoxidative Methane Dehydroaromatization Reactor with a Validated Model for Catalyst Deactivation. *Ind. Eng. Chem. Res.* **2021**, *60* (13), 4903–4918. https://doi.org/10.1021/acs.iecr.0c05493.

(66) Koleva, G.; Galabov, B.; Hadjieva, B.; Iii, H. F. S. An Experimentally Established Key Intermediate in Benzene Nitration with Mixed Acid. *Angew. Chem.* **2015**, 5.

(67) Umbarkar, S. B.; Biradar, A. V.; Mathew, S. M.; Shelke, S. B.; Malshe, K. M.; Patil, P. T.; Dagde, S. P.; Niphadkar, S. P.; Dongare, M. K. Vapor Phase Nitration of Benzene Using Mesoporous MoO3/SiO2 Solid Acid Catalyst. *Green Chem.* **2006**, *8* (5), 488. https://doi.org/10.1039/b600094k.

(68) Sato, H.; Hirose, K. Vapor-Phase Nitration of Benzene over Solid Acid Catalysts (1): Nitration with Nitric Oxide (NO2). *Applied Catalysis A: General* **1998**, *174* (1–2), 77–81. https://doi.org/10.1016/S0926-860X(98)00161-6.

(69) Rosser, W. A.; Wise, H. Thermal Decomposition of Nitrogen Dioxide. *The Journal of Chemical Physics* **1956**, *24* (2), 493–494. https://doi.org/10.1063/1.1742534.

(70) Kosinov, N.; Coumans, F. J. A. G.; Uslamin, E.; Kapteijn, F.; Hensen, E. J. M. Selective Coke Combustion by Oxygen Pulsing During Mo/ZSM-5-Catalyzed Methane Dehydroaromatization. *Angew. Chem. Int. Ed.* **2016**, *55* (48), 15086–15090. https://doi.org/10.1002/anie.201609442.

(71) Nielsen, Torben. Reactivity of Polycyclic Aromatic Hydrocarbons towards Nitrating Species. *Environ. Sci. Technol.* **1984**, *18* (3), 157–163. https://doi.org/10.1021/es00121a005.

(72) Panizza, M. Electrochemical Treatment of Wastewater Containing Polyaromatic Organic Pollutants. *Water Research* **2000**, *34* (9), 2601–2605. https://doi.org/10.1016/S0043-1354(00)00145-7.

(73) Kosinov, N.; Uslamin, E. A.; Meng, L.; Parastaev, A.; Liu, Y.; Hensen, E. J. M. Reversible Nature of Coke Formation on Mo/ZSM-5 Methane Dehydroaromatization Catalysts. *Angew. Chem. Int. Ed.* **2019**, *58* (21), 7068–7072. https://doi.org/10.1002/anie.201902730.

(74) Hsieh, M.; Zhou, Y.; Thirumalai, H.; Grabow, L. C.; Rimer, J. D. Silver-Promoted Dehydroaromatization of Ethylene over ZSM-5 Catalysts. *ChemCatChem* **2017**, *9* (9), 1675–1682. https://doi.org/10.1002/cctc.201700192.

(75) Fürstner, A.; Ackermann, L.; Beck, K.; Hori, H.; Koch, D.; Langemann, K.; Liebl, M.; Six, C.; Leitner, W. Olefin Metathesis in Supercritical Carbon Dioxide. *J. Am. Chem. Soc.* **2001**, *123* (37), 9000–9006. https://doi.org/10.1021/ja010952k.

(76) Abdelsayed, V.; Shekhawat, D.; Smith, M. W. Effect of Fe and Zn Promoters on Mo/HZSM-5 Catalyst for Methane Dehydroaromatization. *Fuel* **2015**, *139*, 401–410. https://doi.org/10.1016/j.fuel.2014.08.064.

(77) Kosinov, N.; Coumans, F. J. A. G.; Uslamin, E. A.; Wijpkema, A. S. G.; Mezari, B.; Hensen, E. J. M. Methane Dehydroaromatization by Mo/HZSM-5: Mono- or Bifunctional Catalysis? *ACS Catal.* **2017**, *7* (1), 520–529. https://doi.org/10.1021/acscatal.6b02497.

(78) Kosinov, N.; Coumans, F. J. A. G.; Li, G.; Uslamin, E.; Mezari, B.; Wijpkema, A. S. G.; Pidko, E. A.; Hensen, E. J. M. Stable Mo/HZSM-5 Methane Dehydroaromatization Catalysts Optimized for High-Temperature Calcination-Regeneration. *Journal of Catalysis* **2017**, *346*, 125–133. https://doi.org/10.1016/j.jcat.2016.12.006.

(79) Lai, Y.; Veser, G. The Nature of the Selective Species in Fe-HZSM-5 for Non-Oxidative Methane Dehydroaromatization. *Catal. Sci. Technol.* **2016**, *6* (14), 5440–5452. https://doi.org/10.1039/C5CY02258D.

(80) Sun, C.; Fang, G.; Guo, X.; Hu, Y.; Ma, S.; Yang, T.; Han, J.; Ma, H.; Tan, D.; Bao, X. Methane Dehydroaromatization with Periodic CH_4-H_2 Switch: A Promising Process for

Aromatics and Hydrogen. *Journal of Energy Chemistry* **2015**, *24* (3), 257–263. https://doi.org/10.1016/S2095-4956(15)60309-6.

(81) Çağlayan, M.; Lucini Paioni, A.; Abou-Hamad, E.; Shterk, G.; Pustovarenko, A.; Baldus, M.; Chowdhury, A. D.; Gascon, J. Initial Carbon−Carbon Bond Formation during the Early Stages of Methane Dehydroaromatization. *Angew. Chem. Int. Ed.* **2020**, *59* (38), 16741–16746. https://doi.org/10.1002/anie.202007283.

(82) Bai, X.; Samanta, A.; Robinson, B.; Li, L.; Hu, J. Deactivation Mechanism and Regeneration Study of Ga–Pt Promoted HZSM-5 Catalyst in Ethane Dehydroaromatization. *Ind. Eng. Chem. Res.* **2018**, *57* (13), 4505–4513. https://doi.org/10.1021/acs.iecr.7b05094.

(83) Mamonov, N. A.; Fadeeva, E. V.; Grigoriev, D. A.; Mikhailov, M. N.; Kustov, L. M.; Alkhimov, S. A. Metal/Zeolite Catalysts of Methane Dehydroaromatization. *Russ. Chem. Rev.* **2013**, *82* (6), 567–585. https://doi.org/10.1070/RC2013v082n06ABEH004346.

(84) Tian, P.; Wei, Y.; Ye, M.; Liu, Z. Methanol to Olefins (MTO): From Fundamentals to Commercialization. *ACS Catal.* **2015**, *5* (3), 1922–1938. https://doi.org/10.1021/acscatal.5b00007.